We thank the reviewers for their constructive comments. In our response, referee comments are indicated in **bold**, with our comments and changes to the manuscript in plain text. In addressing the reviewers' comments, we have added a new figure to the manuscript. Throughout our response, when discussing figures, we give both the original and revised figure number.

Reviewer 1: Bryce Harrop

The manuscript makes use of the available CMIP6 SSP projection simulations to evaluate the impact of changing aerosols on the hydrological cycle over South Asia and East Asia. Despite the lack of clean experiments (non-aerosol differences occur across SSPs), the authors argue that simple and robust patterns appear that fingerprint the role of aerosol uncertainty on changes in precipitation, most notably during the first half of the 21st century. It is often difficult, however, to follow the line of reasoning used in the text of the manuscript when examining the figures presented. I have made a note of several such passages that seem to disagree with what is presented in the figures in the specific comments. There are also several points of discussion in the manuscript relating global scale and regional scale differences, but there is little evaluation presented for which scales are important for which findings. A clearer definition of what constitutes agreement with the hypotheses would make this manuscript much easier to follow. Finally, in addition to discussions about the role of GHGs vs aerosol, there is no mention of land use/land cover change and the impact of its differences between SSPs on rainfall over South Asia or East Asia in this manuscript.

Thank you Bryce for the thoughtful and detailed review. We have added detail to the text throughout the manuscript, which hopefully makes our reasoning clearer. Where you had specific concerns about particular paragraphs, we have addressed them in the manuscript and respond to them directly below.

AR5 suggested that land use forcing was an order of magnitude smaller than that from anthropogenic aerosols, so we didn't consider it in the original manuscript. However, we have now looked into the details of the experiments in CMIP6, and the available literature, and agree that it is important to mention this. We have now included a summary of land use changes in our initial description of the SSPs, and commentary on their potential role in the manuscript.

Where data are available, we have calculated the global mean ERF due to anthropogenic aerosol changes and to land use changes. We have included these values in Table 2, alongside the ERF from greenhouse gas increases, and the Equilibrium Climate Sensitivity. The forcing from land use is much smaller than that due to aerosol. However, we note in the manuscript that it may be of more importance locally.

Specific comments

1. The authors argue that, "If the magnitude of the anomaly decreases monotonically from SSP1-1.9, which has the largest aerosol reduction, to SSP3-7.0, which has a moderate aerosol increase, this indicates that aerosol changes are the main driver of the climate response." When looking at the global emissions of BC and SO2 presented in Figure 1, this seems reasonable, but the same logic appears to be applied regionally in this manuscript. Looking at South Asia during the 2015-2050 period, SO2 emissions are highest for SSP5-8.5 and nearly equal for SSP2-4.5 and SSP3-7.0. How are we meant to disentangle the regional and global scale impacts for this region?

Disentangling regional and global scale impacts is a study in itself, and an interesting one. It wouldn't be possible to do with the type of experiments that we consider here. There are a number of published studies that look at the relative roles of local and remote aerosol emissions for monsoon changes. We now refer to these in the manuscript, and make clear that when we look at the monsoon response in the SSPs we are considering the effect of both local and remote aerosol changes.

2. SSP2-4.5 and SSP5-8.5 are said to have "similar aerosol pathways," and globally that appears to be the case (Fig 1). Again, however, over South Asia, the differences in BC and SO2 emissions between SSP2-4.5 and SSP5-8.5 appear to be as large as their differences relative to SSP3-7.0. This point is raised again in the discussion of Fig 4 where the authors state, "SSP5-8.5 has similar aerosol changes to SSP2-4.5, consistent with the similar changes in emissions (Figure 1)." Given how dissimilar the regional emissions are in Figure 1, it is disconcerting that the AOD pattern for SSP5-8.5 is left off Figure 4, as this would allow readers to accurately see how similar or not the regional emissions are.

We have added the AOD for SSP5-8.5 to Figure 4, and more clearly delineated our discussion of regional and global aerosol when introducing the SSPs.

In our discussion of the results we now refer to the different characteristics of the emission pathways over South Asia compared to the global and East Asian case, and discuss the impact of this in the context of the monsoon changes.

3. Figures 5 and 6 show the model mean responses (as points), as well as their interquartile spread, for global (fig 5) and regional (fig 6) metrics. The temperature responses show noticeable spread between the different pathways, particularly by 2045-2054, but the precipitation responses have far less separation between pathways. I found it difficult to parse what measure the authors use to decide whether precipitation has increased or decreased between pathways. I began by assuming they were referring to the median (which I assume is the horizontal line in each bar). If that were true, then the statement, "Global aerosol reductions in SSP1-1.9 briefly cause this scenario to warm faster than the others considered over Asia and East Asia..." should be changed to refer only to East Asia, as Fig 6a (left panel) does not show a larger median temperature anomaly for SSP1-1.9 than SSP2-4.5. Additionally, the statement, "Over Asia, the largest mean precipitation increase occurs, for all decades, in SSP1-1.9..."is difficult to parse when it isn't clear if the "mean precipitation" is even marked in the figure. Is the bar actually the multi-model mean? If that is true, then the increase in precipitation over Asia is larger in both SSP2-4.5 and SSP5-8.5 than it is in SSP1-1.9. These two figures, and their accompanying text, must be clarified before any rigorous evaluation of the conclusions can be made. I also strongly recommend adding some discussion of when differences between regional precipitation changes at the decadal scale are statistically significant, or at a minimum robust across models.

We have now included a paragraph clarifying the approach used in Figures 5 and 6 (revised Figures 6 and 7). The horizontal bars are the median, and we have now taken care to refer to this consistently in the text, rather than referring to the mean. We now include a discussion of significance and robustness throughout this section. For our sample size, the 95% confidence interval about the median is typically very close to the interquartile range, based on the empirical relation in McGill et al. (1978). To account for the asymmetry in the distribution of models about the median in some cases, we use the interquartile range to determine significance.

4. The cooling over India is argued as the reason for suppressed precipitation in-creases in SSP2-4.5 and SSP5-8.5 relative to SSP1-1.9 and SSP3-7.0, but the cooling in Figure 7 is strongest for SSP3-7.0. How does one reconcile this? On a similar note, why are the temperature anomalies for South Asia and East Asia all positive in Figure 6a when Figure 7 shows cooling for SSP2-4.5, SSP3-7.0, and SSP5-8.5 for2025-2034?

Figure 6 (revised Figure 7) shows an anomaly relative to 1980-2014, so includes a considerable amount of global warming. Figure 7 (revised Figure 8) shows the same for SSP1-1.9. For the other scenarios in Figure 7 (revised Figure 8), we show a difference relative to SSP1-1.9 to try to highlight the differences between the scenarios. This is the reason for the apparent change in sign between Figures 6 and 7 (revised Figures 7 and 8), and we have clarified this in the text and the caption.

We have removed the argument for cooling as the reason for suppressed precipitation since precipitation changes can also lead to temperature changes.

5. The warming and rainfall change patterns for the two individual SSP2-4.5-aer simulations are difficult to compare to the multimodel mean, and even to the rainfall response in Figure S8 (owing to changes in both the range of the colorbar and the colors used). It would be useful to show a direct comparison of the full SSP2-4.5 response to that of SSP2-4.5-aer for each of the two models available so that an assessment can be made for how much the climate responses are indeed driven by aerosols.

This comparison is now included. We show both SSP2-4.5-aer and SSP2-4.5 for MIROC6 in the main text (revised Figures 12 and 13), and SSP2-4.5-aer and SSP2-4.5 for CanESM5 in the supporting information (Supplementary Figures 7 and 8). We now use consistent colours for our precipitation scales throughout the manuscript to facilitate comparison between figures.

6. Figures are too small to be readable when printed, and the quality is so low that they are hard to read even when zoomed in on a computer. Please consider revising with vector graphics or higher DPI raster images. It would be helpful to readers to add an outline of the analysis regions (Asia, S. Asia, and E. Asia) to the map plots. Please maintain a consistent map projection for all map plots. Please also be consistent with colorscales so that metrics can be compared

across figures (e.g., Fig 7 vs Fig 11, or Fig 9 vs Fig 11). Finally, please consider changing Fig 4c to be MMM-MODIS so that it is consistent with the caption.

We have provided both vector and higher DPI raster images to ACP, and added outlines of the analysis regions to Figure 4.

All regional plots now use the same domain, except for Figure 3 (revised Figure 4), S1, and S2, where we use a slightly smaller domain. These figures show a comparison to APHRODITE, which has a limited data domain.

The different magnitudes in Figures 7-11 (revised manuscript: Figures 8-12) made it difficult to use exactly the same colour scale throughout. However, we have now standardised the type of colour scale used for each variable, so that temperature is now blue:yellow:red, precipitation is red:white:blue, and sea level pressure is brown:white:green throughout.

We have made the suggested change to Figure 4c (revised Figure 5c).

Technical corrections

Page 2, line 34, "AA" is not defined Page 4, line 7 typo "has yet to be emerge" Page 6,line 6 typo "present - day" Figure 2 caption typo "180-2014" Figure 7, there is a change in font between subpanels

All now corrected, thank you.

References

Robert McGill, John W. Tukey and Wayne A. Larsen. Variations of Box Plots, The American Statistician, Vol. 32, No. 1 (Feb., 1978), pp. 12-16

Reviewer 2

This study investigates the possible influences of different aerosol reductions in the future on the global and Asia surface temperature and rainfall. The topic is quite important, but the method they took may have some problems, at least for some conclusions. Their writing is very unclear (with many typos, which greatly affect the reading experience) and very hard to follow. At the same time, the figures are so small and so unclear (also the captions) that I try my best to understand what they showed. Besides these, I still have several major comments and I don't think this manuscript can be accepted unless all these concerns are well addressed.

We thank the reviewer for their comments and are sorry to hear that they found our writing unclear. We have corrected the typos identified by both reviewers, made changes to the text to further improve the clarity. We have added more detail about our methodology. We have also added extra detail to the captions of Figures 5, 6, 7, 8, 9, and 10, and included either higher resolution or vector versions of all figures. We have also addressed the reviewer's detailed comments in the manuscript, and provide responses for those separately below.

Major comments:

1. Due to the lack of clean experiments, the guidance to distinguish the relative importance of GHG and aerosol forcing in this study is that different scenarios may be similar in one forcing change, while very different in the other forcing change. This seems plausible, but the question is whether the other forcings (e.g.,land use) keep unchanged in different scenarios. I guess probably not. So the question is whether they are important or not for the main conclusion drawn here. I think the authors should seriously think about it and do some analysis on it.

The SSPs do include a range of land use changes in addition to a range of aerosol pathways. We have now included a summary of land use changes in our initial description of the SSPs, and commentary on their potential role in our results. There is a limited amount of literature available that already compares the relative roles of anthropogenic aerosol and land use changes in monsoon changes, and we now refer to this in the text. This work suggests that the response to anthropogenic aerosol changes is larger than the response to land use changes over China, but that land use changes may be important over India.

Where data are available, we have calculated the global mean effective radiative forcing (ERF) due to anthropogenic aerosol changes and to land use changes. We have added these values to the manuscript in Table 2, alongside the ERF from greenhouse gas increases, and the Equilibrium Climate Sensitivity. The forcing from land use is much smaller than that due to anthro-

pogenic aerosol. However, as we now note in the discussion, it may be of more importance locally. Overall, it looks like the land use changes will drive monsoon changes of the same sign as the aerosol driven changes, and we have also noted this in the manuscript.

Given that the forcing from land use changes are so small compared to the forcing from anthropogenic aerosol, we think it would be distracting to include analysis beyond a comparison of the radiative forcings and a discussion of the relevant literature in this paper.

2. From Fig. 5, it seems that for the global mean precipitation and hydrological sensitivity, the responses of most models are close to each other, except two models with totally opposite signs (one with large positive value and the other with large negative value). Could you do more analysis on these two models? With the same aerosol emission, how can these two models produce totally opposite results? To me, I know the aerosol forcing has large uncertainty (should affect the results in a quantitative way), but in a qualitative way, it should be the same result at least at the global mean. Hence, it quite surprises me. In Fig. 6, it seems that over Asia, the uncertainty is smaller, at least not opposite.

The outlying models in Figure 5, and the large opposite responses from two models in Figure 5c, are mainly the result of our choice to show anomalies relative to 1980-2014, rather than large differences in absolute values across the models. These anomalies for each SSP include a large amount of global warming, and the difference between the outlying models is largely a reflection of different climate sensitivities, rather than differences in the response to aerosol forcing. For each scenario, the outlying models are the same in each case, so have no influence on the relative differences between the scenarios.

Figure 1 of this response shows the temperature time series that are used in Figure 5 (revised Figure 6). SSP2-4.5 is used as an example. Panel (a) shows the absolute values of global-mean JJA-mean near-surface temperature. The outlying models from Figure 5 (revised Figure 6) are highlighted with bolder lines. Panel (b) shows the same data as anomalies relative to 1980-2014, which is what we show in the paper. Comparison of the two panels demonstrates that the models are not unusual in their mean climate, or the sign of the trend, but do warm relatively more (or less) than the other models between 1980 and 2020.

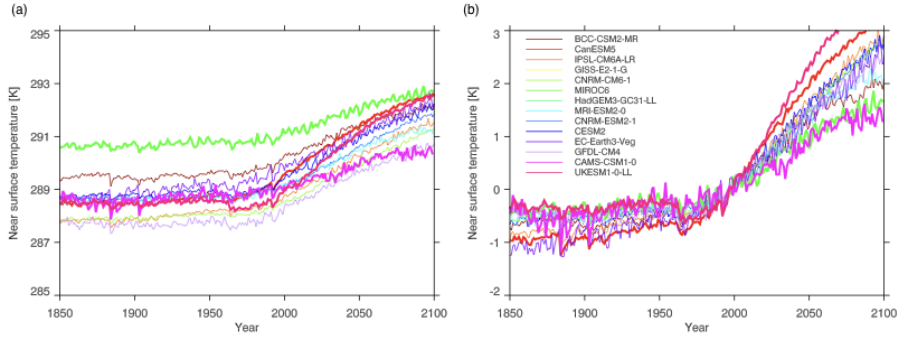

Figure 1. (a): Annual-mean global-mean temperature time series for the historical simulation and SSP2-4.5. (b): The same data as shown in panel (a), but presented as an anomaly relative to 1980-2014. Results presented in the manuscript are anomalies relative to 1980-2014, which causes the models with relatively large or relatively small trends over this period to appear as outliers.

We have done some further analysis of the outlying models from Figure 5 (revised Figure 6), as suggested by the reviewer. Globally, the low outliers are MIROC6 (temperature) and CAMS-CSM1-0 (precipitation), while the high outliers are EC-Earth-Veg, UKESM, and CanESM5 (temperature) and UKESM (precipitation). These models are those with the lowest and highest climate sensitivities in our subset, consistent with them having the smallest and largest trends over 1980-2014 (as shown in Figure 1 of this response). These points are now noted in the manuscript. Maps of the precipitation responses in the individual models are shown in Figure S10.

Specific comments:

1. Page2L35: Why is this case? It is hard to understand. It is better to provide an explanation here. We now explicitly state that future warming is driven by a combination of positive radiative forcing from greenhouse gas increases and positive radiative forcing from anthropogenic aerosol decreases, so that a weaker aerosol forcing results in a more moderate warming.

2. Page3L13: full->fully Done

3. Page3L14: add aperiod. Done

4. Page7L3-4: You should clearly state this in the figure caption to make sure each figure can be understood from the figure itself. Details of the quantities shown in the box plots have been added to the captions for Figures 5 and 6 (revised Figures 6 and 7).

6. Page7L18: Please add "partly". I don't think aerosol forcing explains all the weakening of Asian summer monsoon. Changed to 'largely'. We accept that a single forcing is unlikely to explain all of the weakening, but there is good evidence that aerosol forcing is the dominant driver (relevant papers cited in manuscript).

6.Page7L30: remove "the" This sentence has been rewritten.

7. Section 4.1: I don't think it is suitable to compare the SSP2-4.5-aer simulations from two models with SSP2-4.5 simulations from all models. You should compare these two simulations from the same model. This comparison is now included. We show both SSP2-4.5-aer and SSP2-4.5 for MIROC6 in the main text (Figures 12 and 13), and SSP2-4.5-aer and SSP2-4.5 for CanESM5 in the supporting information (Figures S7 and S8).

Additional changes not requested by the reviewers

There was a problem with the secondary organic aerosol in the CESM SSPs and the data has been withdrawn: https://errata.es-doc.org/static/view.html?uid=eb69632c-a6e2-7667-a112-a98b7745e2ea We have removed these simulations from our analysis.

In the submitted version of the manuscript there were data points with a temperature anomaly of 0K in Figure 5a. These were erroneous, and have been corrected in the revised version (Figure 6a).

As part of our attempt to improve the readability of the manuscript, we have replaced the JJA mean interhemispheric temperature gradient originally shown in Figures 2b and 5d with the annual mean, making it consistent with the other panels in the figure. We had originally included JJA here to give a closer link to the monsoon results discussed later in the manuscript. However, the pattern of the response across the SSPs is similar in both seasons, and the use of the annual mean for this panel means that all discussion in Section 3 is for the same season. The panels from Figure 5 (revised Figure 6) for the annual mean (a) and JJA mean (b) are shown in Figure 2 of this response. There is no qualitative difference between them when comparing the relative position of the median across SSPs.

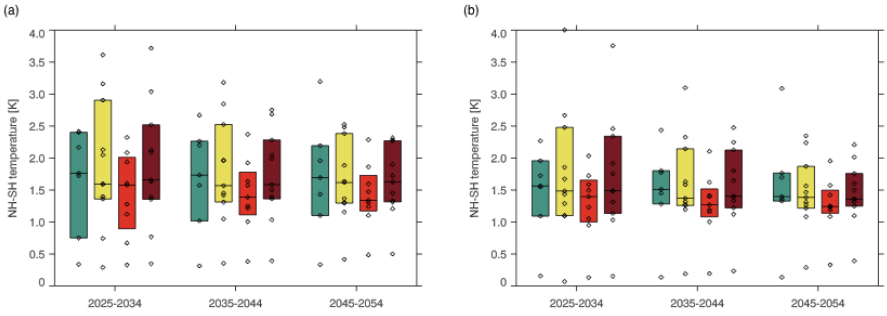

Figure 2. (a): Annual-mean interhemispheric temperature gradient anomalies relative to 1980-2014 from SSP1-1.9, 2-4.5, 3-7.0, and 5-8.5 (as shown in the revised manuscript). (b): As for panel (a), but for JJA (as shown in the original manuscript).

Accelerated increases in global and Asian summer monsoon precipitation from future aerosol reductions

Laura J. Wilcox[1,2], Zhen Liu[3], Bjørn H. Samset[4], Ed Hawkins[1,2], Marianne T. Lund[4], Kalle Nordling[5], Sabine Undorf[6], Massimo Bollasina[3], Annica M. L. Ekman[6], Srinath Krishnan[6], Joonas Merikanto[5], and Andrew G. Turner[1,2]

[1]National Centre for Atmospheric Science, UK
[2]Department of Meteorology, University of Reading, Reading, UK
[3]School of Geosciences, Grant Institute, University of Edinburgh, Edinburgh, UK
[4]CICERO Center for International Climate and Environmental Research, Oslo, Norway
[5]Finnish Meteorological Institute, Helsinki, Finland
[6]Department of Meteorology, Stockholm University, Stockholm, Sweden

Correspondence: Laura Wilcox l.j.wilcox@reading.ac.uk

Abstract. There is ~~large uncertainty in~~ a large range of future aerosol emissions scenarios explored in the Shared Socioeconomic Pathways (SSPs), with plausible pathways spanning a range of possibilities from large global reductions in emissions ~~to~~ by 2050 to moderate global increases over the same period. Diversity in emissions across the pathways is particularly large over Asia. Rapid reductions in anthropogenic aerosol and precursor ~~emission reductions~~ emissions between the present day and the 2050s lead to enhanced increases in global and Asian summer monsoon precipitation relative to scenarios with weak air quality policies. However, the effects of aerosol reductions don't persist ~~in precipitation~~ to the end of the 21st century ~~,~~ ~~when~~ for precipitation, when instead the response to greenhouse gases dominates differences across the SSPs. The relative magnitude and spatial distribution of aerosol changes is particularly important for South Asian summer monsoon precipitation changes. Precipitation increases here are initially suppressed in SSPs 2-4.5, 3-7.0, and 5-8.5 relative to ~~SSP 1-1~~SSP1-1.9 ~~and 3-7.0~~ when the impact of ~~East Asian~~ remote emission decreases is counteracted by ~~that due to~~ continued increases in South Asian emissions.

1 Introduction

Anthropogenic aerosols can affect climate either by scattering or absorbing solar radiation, or by changing cloud properties (Boucher et al., 2013). Overall, aerosols have a global-mean cooling effect, manifested, for example, in a slower rate of global warming in the mid twentieth century ~~concurrently with the~~ concurrent with rapid increases in aerosol burden (Wilcox et al. (2013); Jones et al. (2013); Hegerl et al. (2019)). This has raised the question of whether the warming associated with present-

day and future reductions in anthropogenic aerosol might exacerbate the climate impacts brought about by continued increases in greenhouse gas ~~emissions alone~~(GHG) emissions.

Many studies have demonstrated the potential for an enhanced future warming from aerosol reductions in global climate models driven by plausible reductions in the emissions of anthropogenic aerosol and their precursors (e.g. Chalmers et al. (2012); Levy et al. (2013); Rotstayn et al. (2013); Acosta Navarro et al. (2017))~~, which in recent years~~. In recent years, emission scenarios have typically been taken from either the Representative Concentration Pathways (RCPs; Moss et al. (2010); van Vuuren et al. (2011)) used in the 5th Coupled Model Intercomparison Project (CMIP5; Taylor et al. (2012)), or the more diverse ECLIPSE (Klimont et al., 2017) aerosol pathways: CLE (Current LEgislation), and MFR (Maximum Feasible Reductions). Estimates based on transient simulations with CMIP5 generation models suggest that future aerosol reductions may result in warming of up 1.1K in addition to any ~~greenhouse gas (GHG)-driven~~ GHG-driven warming (e.g. Rotstayn et al. (2013); Levy et al. (2013); Acosta Navarro et al. (2017)). This ~~means~~ indicates that reduced anthropogenic aerosol emissions may account for up to half of the total warming by 2100 in scenarios with moderate GHG increases. Similar magnitudes are also seen in studies using equilibrium experiments (Kloster et al., 2010), reduced complexity models (Hienola et al., 2018), and studies assuming a complete removal of anthropogenic aerosol (Samset et al. (2018); Nordling et al. (2019)).

The important role of anthropogenic aerosol in driving precipitation changes has also been documented, including the possible contribution to the spin down in the global water cycle in the mid-twentieth century (Liepert et al. (2004); Wilcox et al. (2013); Wu et al. (2013)). A greater response of global mean precipitation to anthropogenic aerosol changes compared to GHGs is expected since ~~shortwave drivers have~~ aerosol has a stronger effect on atmospheric shortwave transmissivity, and thus a stronger influence on ~~the water cycle~~ radiative energy imbalance (e.g. Liepert et al. (2009); Andrews et al. (2010); Rotstayn et al. (2013); Samset et al. (2016); Liu et al. (2018)). The apparent hydrological sensitivity (% change in precipitation divided by absolute change in temperature; Fläschner et al. (2016)) for anthropogenic aerosol is twice that for GHGs (Kloster et al. (2010); Salzmann (2016); Samset et al. (2016)). This enhanced sensitivity means that anthropogenic aerosol reductions might be expected to play a relatively more important role in future increases in global precipitation for a given temperature change. Several studies using CMIP5 models estimate an increase in global mean precipitation between 0.09 and 0.16 mm day^{-1} by 2100 from aerosol reductions (e.g. Levy et al. (2013); Rotstayn et al. (2013); Westervelt et al. (2015)).

~~Their heterogeneous forcing distribution and influence on circulation patterns mean that the~~ The effects of future aerosol reductions are likely to be felt more strongly at regional ~~than global scale~~rather than global scales due to their heterogeneous forcing distribution and strong influence on circulation patterns. Previous work has identified relatively large temperature increases over Europe (Sillmann et al., 2013), the Arctic (Acosta Navarro et al., 2016), and East Asia (Westervelt et al., 2015), compared to the global mean response. For precipitation, the regional response is particularly pronounced for the Asian summer monsoon (Levy et al. (2013); Westervelt et al. (2015); Acosta Navarro et al. (2017); Bartlett et al. (2018); Samset et al. (2018)). Here, precipitation is ~~sensitivie~~ sensitive to changes in remote aerosol through its control on the Interhemispheric Temperature Gradient and Inter Tropical Convergence Zone (ITCZ) location and the atmospheric wave pattern over Eurasia, and to local aerosol changes, which further modify the local monsoon circulation (Polson et al. (2014); Dong et al. (2016); Guo et al. (2016); Shawki et al. (2018); Undorf et al. (2018)). ~~Asia will also~~ Importantly, Asia will undergo the largest anticipated

future changes in aerosol amounts worldwide (Lund et al. (2018); Scannell et al. (2019)), and is thus a region likely to see an anthropogenic aerosol influence on near-future precipitation trends.

Despite evidence that anthropogenic aerosols influence temperature and precipitation, quantification of the associated changes is hindered by several compounding uncertainties. The degree by which ~~AA~~ anthropogenic aerosol reductions enhance future climate change is model dependent~~, with models featuring~~ . Models with weaker historical aerosol forcing generally ~~predicting more~~ have weaker positive radiative forcing from future aerosol reductions, and therefore predict relatively moderate global mean warming (Gillett and Von Salzen (2013); Westervelt et al. (2015)) and moderate precipitation increases due to ~~aerosol reductions in future (Rotstayn et al., 2015)~~future aerosol reductions (Rotstayn et al., 2015), compared to models with larger aerosol forcing. The uncertainty in aerosol radiative forcing itself is currently the largest source of uncertainty in estimates of the magnitude of the total anthropogenic forcing on climate, with the most recent estimate producing a 68% confidence interval from ~~~~-1.60 to ~~~~-0.65 W m^{-2} (Bellouin et al., 2019). This is comparable to the range simulated by CMIP5 models: -1.55 to -0.68 W m^{-2} (Zelinka et al., 2014). The effect of this uncertainty on regional climate projections may be further enhanced by feedbacks from ~~circulation changes (Wilcox et al. , submitted).~~ atmospheric circulation changes (Nordling et al., 2019). The compensating effects from the response to different near-term climate forcers also ~~adds to~~ increases the uncertainty in multi-decadal projections, with future changes in methane and nitrate aerosol having the potential to moderate future temperature enhancements from decreases in anthropogenic aerosol (Bellouin et al. (2011); Shindell et al. (2012); Pietikäinen et al. (2015)). At regional scales, changes in land use may also play an important role (Singh et al., 2019b).

In opposition to the CMIP5-generation findings summarised above, Shindell and Smith (2019) recently dismissed the possibility that future aerosol reductions might lead to rapid increases in the magnitude or rate of global-mean warming, even in scenarios with aggressive clean air policies, based on simulations with a reduced-complexity impulse response model (Smith et al., 2018). Yet, this conclusion may not hold when using a ~~full~~ fully coupled GCM and when investigating changes beyond global mean temperature. Even if the short atmospheric residence time of anthropogenic aerosol ~~possibly~~ potentially makes their effects negligible on centennial timescales, they are likely important for regional and global climate over the next few decades. This is ~~particularly~~ especially the case for Asia where large aerosol emission changes are anticipated, and where aerosol has played an important role in historical changes, in particular for precipitation. In this study, we examine state-of-the-art models and scenarios in CMIP6 and make the case for a potential enhancement of increases in global and Asian temperature and precipitation on a 20-30 year time horizon due to removal of anthropogenic aerosol. Such an effect is ~~of particular importance for adaptation measures~~an important consideration for adaptation and mitigation strategies.

2 Data and methods

2.1 Models and experiments

We use data from the CMIP6 (Eyring et al., 2016) historical experiment (1850-2014) and four future scenarios following Shared Socioeconomic Pathways (SSPs) 1-1.9, 2-4.5, 3-7.0, and 5-8.5 (O'Neill et al. (2016); Rao et al. (2017); Riahi et al. (2017)), which sample a range of aerosol pathways. At the time of writing, data were only available for between 6 and 14 models for

the variables and experiments we consider. The data used in this study are summarised in Table 1. All available data is used for each experiment, and model means are used in multi-model comparisons, except where otherwise stated. Many CMIP6 models include improved representation of aerosol microphysics and aerosol-cloud interactions compared to CMIP5, such as internal mixing and heterogeneous ice nucleation (e.g. Bellouin et al. (2013); Mulcahy et al. (2018); Kirkevåg et al. (2018); Wyser et al. (2019)). ~~We use data from the historical experiment (1850-2014) and four future scenarios following Shared Socioeconomic Pathways (SSPs) 1-1.9, 2-4.5, 3-7.0, and 5-8.5 (O'Neill et al. (2016); Rao et al. (2017); Riahi et al. (2017)), which sample a range of aerosol pathways.~~

The SSPs used in CMIP6 sample a far greater range of uncertainty in future aerosol and precursor emissions than the RCPs used in CMIP5 (Scannell et al. (2019); Lund et al. (2018)). Partanen et al. (2018) highlighted the importance of uncertainty in aerosol emission pathways for the potential enhancement of global temperature increases from anthropogenic aerosol reductions. The CMIP5 RCPs 2.6-8.5 sampled only a limited range of this emission uncertainty, with an associated ~~0.18K~~ difference in global mean temperature of no more than 0.18K throughout the twenty-first century. Contrasting aerosol pathways spanning a wider range of emission uncertainty resulted in a difference of up to 0.86K ~~difference~~(in 2061). The SSPs span most of this wider range of emissions pathways explored by Partanen et al. (2018). They ~~consider~~ include large, rapid reductions in aerosol and precursor emissions in SSP1-1.9, more moderate reductions (comparable to the RCPs) in SSP2-4.5 and SSP5-8.5, and continued increases in the coming decades in SSP3-7.0 (see Figure 1). Much of the spread in global emission pathways comes from diversity over Asia and North Africa (Lund et al., 2018).

In our analysis, we compare the future decadal-mean climate changes to the present day (1980-2014) across SSPs 1-1.9, 2-4.5, 3-7.0, and 5-8.5. We focus on the period up to the 2050s, when aerosol emission uncertainty is largest, but the full range of uncertainty in greenhouse gas (GHG) emissions has yet to ~~be~~ emerge (Figure 1). However, the changes in GHG emissions in this period are not negligible, and the ~~anomalies~~ emerging modelled climate responses we show include the effects of changes in both anthropogenic aerosols and greenhouse gases. ~~This precludes the quantification of the~~ The SSPs also consider a range of land use scenarios, with extensive and moderate deforestation in SSP3-7.0 and SSP5-8.5 respectively, little change in forest cover in SSP2-4.5 before 2050, and large-scale afforestation in SSP1-1.9 (O'Neill et al., 2016). Where data are available, we have provided the global-mean annual-mean effective radiative forcings (ERFs) due to historical changes in anthropogenic aerosols, GHGs, and land use changes in Table 2, as an indicator of the relative importance of these changes on centennial timescales. Typically GHG forcing over the historical period is 2-3 times larger than aerosol forcing, which is in turn an order of magnitude greater than land use forcing. However, ERFs over the historical period are not always good predictors of behaviour on shorter timescales. For example, aerosol can be more important than GHGs for decadal-scale changes (e.g. Wilcox et al. (2013)).

Since multiple forcing agents vary simultaneously in the SSPs, it is not possible to quantify the respective effects of aerosol and ~~greenhouse gas changes, but does not prevent the identification of the~~ GHG changes, although the main driver of ~~the anomaly . If the magnitude of the anomaly decreases monotonically from~~ an anomaly can still be identified. Consider the global emission changes shown in Figure 1. SSP1-1.9 ~~, which~~ has the largest aerosol ~~reduction, to~~ and GHG emission reduction, while SSP3-7.0 ~~, which~~ has a moderate ~~aerosol increase (Figure 1~~increase in aerosol emissions (reverse climate response to

SSP1-1.9) and moderate increase in GHG emission (enhanced climate response to SSP1-1.9). If the magnitude of the climate response to these changes decreases monotonically from SSP1-1.9 to SSP3-7.0 (Figure 2), this indicates that aerosol changes are the main driver of the climate response. Further confirmation of aerosol as the main driver is gained from the comparison of the anomalies in SSP2-4.5 and SSP5-8.5, which have similar aerosol pathways, but very different greenhouse gas pathways (Figure 1, Figure 2). If the climate response in these two scenarios is similar, then the greenhouse gas influence has yet to emerge over the aerosol signal. As the differences in greenhouse gas emissions between the two scenarios increase, a larger response is expected in SSP5-8.5, which has large increases in global GHG emissions compared to very moderate increases in SSP2-4.5 (Figure 1). In cases where GHGs are the main driver of the ~~anomaly, the responses~~ response, the magnitude will increase monotonically from SSP1-1.9 to SSP5-8.5 (Figure 2).

In Section 4.1, we use an additional DAMIP (Detection and Attribution Model Intercomparison Project; Gillett et al. (2016)) experiment, SSP2-4.5-aer. This differs from the companion SSP2-4.5 in that only aerosol emissions are evolving while all other forcings are held constant at their 1850 levels. This scenario allows the response to anthropogenic aerosols to be seen in isolation from the response to greenhouse gas changes and may thus provide support to any conclusion drawn from the analysis of the SSP2-4.5 experiment. Data for this experiment is so far only available for two models, CanESM5 and MIROC6 (Shiogama (2019); Swart et al. (2019a)). In this analysis, decadal mean anomalies are again presented relative to the present day (1980-2014). However, in this case, the present day is necessarily defined based on the historical-aer simulation (a historical simulation where only anthropogenic aerosol and precursor emissions are transient, also included in DAMIP).

2.2 Present day model evaluation

Here, we use a number of observation and reanalysis datasets to present a broad evaluation of the performance of CMIP6 models in reproducing present day (1980-2014) climatologies and linear trends in global temperature and precipitation, the interhemispheric temperature gradient, and Asian summer monsoon. Global temperature observations are taken from GISTEMP v4 (Hansen et al. (2010); Lenssen et al. (2019)), the Goddard Institute for Space Studies gridded dataset, which is based on GHCN v4 over land (Global Historical Climatology Network; Menne et al. (2018)) and ERSST v5 over ocean (Extended Reconstructed Sea Surface Temperature; Huang et al. (2017)). GISTEMP is provided as anomalies relative to 1951-1980 on a $2^\circ \times 2^\circ$ grid. For global precipitation, data from the Global Precipitation Climatology Project (GPCP; Adler et al. (2003)) are used on a $2.5^\circ \times 2.5^\circ$ grid. GPCP combines gauge- and satellite-based observations over land with satellite observations over ocean. Since there can be large discrepancies between precipitation observations from different sources (Collins et al. (2013); Sperber et al. (2013); Prakash et al. (2015)), we use a number of datasets in our evaluation of the Asian summer monsoon. Precipitation observations over land are also taken from APHRODITE (Asian Precipitation - Highly-Resolved Observational Data Integration Towards Evaluation; Yatagai et al. (2012)) and the Global Precipitation Climatology Centre (GPCC; Schneider et al. (2014)). APHRODITE contains data from a dense network of rain gauges and is used at $0.25^\circ \times 0.25^\circ$ resolution, within the domain bounded by 60°E, 150°E, 15°S, and 55°N. GPCC also provides gauge-based data, but at a reduced horizontal resolution ($0.5^\circ \times 0.5^\circ$) compared to APHRODITE. We also show precipitation from CMAP (Climate Prediction Centre Merged Analysis of Precipitation; Xie et al. (1996); Xie et al. (1997)), which blends satellite and gauge-based estimates with

NCEP/NCAR reanalysis precipitation. The atmospheric circulation plays an important role in the distribution of Asian summer monsoon precipitation, so we also compare upper- and lower-tropospheric winds from CMIP6 models to ERA-Interim (Dee et al., 2011).

The global-mean annual-mean temperature anomaly from GISTEMP falls within the range of the CMIP6 ensemble during the historical period (Figure 3a). However, most models overestimate the rate of recent warming (Figure 3a, e). The interhemispheric temperature gradient (Northern Hemisphere - Southern Hemisphere) anomalies are also consistent in GISTEMP and CMIP6 (Figure 3b), although the models generally have anomalies that are more ~~postitive~~ positive than seen in the observations. Most ~~model members~~ models reproduce the negative trend in the interhemispheric temperature gradient in 1950-1974 (Figure 3e), which is associated with a global increase in anthropogenic aerosol and a weakening of the global monsoon (e.g. Polson et al. (2014)). ~~The~~ Most models also capture the positive trend in interhemispheric temperature gradient since 1980-2014 when rates of change in the global aerosol burden were relatively small (Figure 3e).

All models simulate an increase in global-mean annual mean precipitation since 1980, and most model members simulate larger trends than observations (Figure 3c,e). The observed trend in Asian (67.5-145°E, 5-47.5°N) summer (June-August, JJA) precipitation is small compared to interannual variability, and this is reflected in large uncertainty in the sign of the modelled trend (Figure 3d, e).

~~Modelled global mean precipitation for the period 1980-2014 is too large compared with GPCP data, primarily due to excessive tropical precipitation (Figure 3c). The models generally overestimate midlatitude precipitation trends, and show no consensus on the sign of the trend in the SH tropics and subtropics (Figure 3d). However, the models do capture the time evolution of the global precipitation anomaly.~~

Compared to APHRODITE, the CMIP6 ensemble mean underestimates summer ~~(June-September, JJAS)~~ monsoon precipitation amount over India, and overestimates it over the Tibetan Plateau and the ~~Indo-China~~ Indochina peninsula (Figure 4a, c). The magnitude of the bias between the CMIP6 multi-model mean and APHRODITE is comparable to the magnitude of the difference between observational datasets over northeast China and India, but ~~model bias over~~ the model biases over the Tibetan Plateau and ~~Indo-China peninsula is~~ the Indochina peninsula are relatively large (Figure 4). The modelled meridional component of the monsoon circulation at 850hPa is too strong over the Equatorial Indian Ocean, while the flow over the Bay of Bengal, and the extension of the circulation into China, is too weak (Figure 4e). This pattern is seen in almost all models, and is highlighted in the comparison of the zonal and meridional components of the 850 hPa wind in CMIP6 and ERA-Interim in Figure 4f. This weak extension of the summer monsoon into eastern China, with an anomalously strong extension into the subtropical west Pacific (Figure 4e), is consistent with the pattern of differences between CMIP5 models and observations (Sperber et al., 2013)~~, although~~ . Nevertheless, the CMIP6 models are more skilful in their representation of the Indian summer monsoon compared to CMIP5 (Gusain et al., 2020).

While aspects of the CMIP6 multi-model mean summer monsoon compare well with observations, and the multi-model mean performs better than the individual models, there is a large inter-model diversity in the monsoon ~~characteristics exhibited~~ precipitation and atmospheric circulation (summarised in Figure 4f; maps of ~~present - day~~ present-day means, and anomalies compared to ~~observations~~ both APHRODITE and GPCP are shown for individual models in Supplementary Figures S1-S5).

Of the models we will consider on an individual basis in Section 4.1, CanESM5 has a small regional mean precipitation bias, but a weak pattern correlation, compared to APHRODITE. It has a particularly large dry bias over India, with less than 3 mm day^{-1} in the seasonal mean, and a relatively large excess of precipitation over the Tibetan Plateau and into China. MIROC6 performs relatively well over land, but has excessive precipitation west of India (Supplementary Figures 1, 2, 4, 5). Such biases may affect the pattern of the precipitation anomaly in the SSPs relative to the present day (Wilcox et al., 2015).

Aerosol optical depth (AOD) is a measure of the extinction of solar radiation due to scattering and absorption by an aerosol layer. Comparison of ~~simulated~~ 550nm AOD from CMIP6 and MODIS (Remer et al. (2008); Platnick (2015)) ~~550nm aerosol optical depth~~ for the common 2002-2014 period ~~,~~ shows that models underestimate AOD over much of the ~~tropics and NH mid-high latitudes~~NH outside Asia, and overestimate it in the SH midlatitudes (Figure 5a-c). This pattern is common across models, with the ~~exception of CanESM5, which overestimates AOD over Eurasia compared to MODIS~~ some exceptions over Asia (Supplementary Figure S6 shows the comparison between AOD from individual models and MODIS). CanESM5 overestimates AOD over Eurasia, and northern China in particular, compared to MODIS. UKESM1-0-LL and IPSL-CM6A-LR have more moderate overestimates of AOD ~~gives an indication of the amount of aerosol in a given location, but does not give an indication of aerosol forcing. It gives no indication of particle number, as AOD is influenced by the optical properties of those particles, and no indication of aerosol-cloud interactions, which account for the majority of aerosol forcing in models (Zelinka et al., 2014)~~over parts of Asia. However, both models underestimate AOD over eastern China, where very high AOD is seen in MODIS.

2.3 Future anthropogenic aerosol changes

In all SSPs the largest AOD changes are over Asia (Figure 5~~d-f~~d-g), consistent with the changes in aerosol and precursor emissions (Figure 1). Future changes in AOD are characterised by global decreases in SSP1-1.9, with the exception of an initial increase over South Asia, and positive anomalies relative to 1980-2014 over the Tibetan Plateau and southern Africa, which may ~~be dust~~ have a dust component (Figure 5d). AOD changes are characterised by regional contrasts in SSP2-4.5 and SSP5-8.5, with an overall decrease in the NH contrasted with an increase in the SH, and large decreases over East Asia against large increases over South Asia until the 2030s (Figure 5e). This Asian dipole pattern is persistent in SSP2-4.5 and SSP5-8.5 and strengthens from the present until the 2040s. In ~~this pathway,~~ these pathways, aerosol and precursor emission are similar, with the large increases in South Asian AOD ~~are~~ predominantly driven by increases in SO_2 emissions ~~. SSP5-8.5 has similar aerosol changes to SSP2-4.5, consistent with the similar changes in emissions~~ (Figure 1). Emissions of black carbon in South Asia do follow different trajectories in the two pathways, but black carbon accounts for a smaller proportion of the total emission (Figure 1), and thus the total AOD. The final scenario we consider, SSP3-7.0, ~~also~~ again contrasts widespread decreases in NH AOD against increases in the SH (Figure 5f). However, this scenario also includes large aerosol and precursor emission and AOD increases over East Asia and particularly South Asia. These increases are driven predominantly by SO_2 over South Asia, but have a BC contribution over East Asia (Figure 1). ~~This pattern persists~~As East Asian SO_2 is roughly constant between 2014 and 2050 in SSP3-7.0, much of the large positive anomaly there is a reflection of the large positive

trend in AOD between 1980 and 2014.The AOD pattern in SSP3-7.0 persists through the three periods shown in Figure 5, but the East Asian increase starts to weaken by 2050 (Figure 1).

3 Global response

~~Global mean annual mean temperature~~Global-mean annual-mean temperature, precipitation, and hydrological sensitivity anomalies for 2025-2034, 2035-2044, and 2045-2054 relative to 1980-2014 are shown in Figure 6~~a~~, along with interhemispheric temperature gradients for the same periods. The boxes show the interquartile range, based on ~~model mean responses, with individual model-mean responses overlaid. For each period, the responses~~ the mean response from each individual model. Individual model responses are overlaid, and the horizontal bar shows the median. The 95% confidence interval (95% CI) about a median can be found from the empirical relationship:

$$95\%CI = \pm\frac{1.57 \times IQR}{\sqrt{n}} \quad (1)$$

where IQR is the interquartile range and n is the number of points (McGill et al., 1978). For the sample size used in this work (n=11), $\frac{1.57}{\sqrt{n}} \approx 0.5$, so we use the interquartile range to determine significance, rather than assuming that the confidence interval is symmetric about the median.

For each period shown in Figure 6a, the global mean temperature anomalies are broadly ordered according to their GHG pathway, and diverge with time in a similar fashion to GHG emissions (Figure 1a, Figure 2). By 2045-2054, SSP2-4.5, 3-7.0, and 5-8.5 anomalies relative to 1980-2014 are significantly larger than those for SSP1-1.9. The anomaly from SSP5-8.5 is also significantly larger than that from SSP2-4.5. This suggests that anthropogenic aerosol plays ~~at most~~ a limited role in the evolution of global mean near-surface temperature on these timescales, supporting the conclusions of Shindell and Smith (2019). However, as ~~discussed later~~will be discussed in Section 4, it does play a role in the pattern and magnitude of regional temperature ~~changes~~change. Importantly, anthropogenic aerosol is the main driver of trends in the interhemispheric temperature gradient until 2050 ~~,~~ (Figure 6d, Figure 2), which has a strong control on ITCZ position and the global monsoon, and thus regional precipitation~~(Figure 6d)~~. There is a large spread in interhemispheric temperature gradient anomalies across models, consistent with the large uncertainty in historical trends (Figure 3e), but a monotonic increase in the magnitude of the anomaly from SSP3-7.0 to SSP1-1.9 is present in all three future periods. The dominant role of anthropogenic aerosol is further supported by the comparable magnitude of anomalies in SSP2-4.5 and SSP5-8.5 (Figure 6d, Figure 2).

There is a clear aerosol-driven signal in future increases in global mean precipitation and hydrological sensitivity (Figure 6b, c, Figure 2). There is the suggestion of the beginning of a shift towards GHGs as the dominant driver of precipitation increases in 2050, where the SSP1-1.9 anomaly is marginally smaller than in SSP2-4.5, but this is not seen in hydrological sensitivity. ~~where the~~ SSP1-1.9 ~~anomaly is marginally smaller than in SSP2-4~~has significantly larger hydrological sensitivity anomalies relative to 1980-2014 than the other SSPs in all periods shown in Figure 6c (except 5-8.5 in 2025-2034), and remains larger throughout the 21st century (not shown). GHGs are the main driver of global precipitation change by the end of the 21st century (not shown).

A number of prominent outliers can be seen in Figure 6. These points are not indicators of uncertainty in the response to anthropogenic aerosol emissions: for each variable the outlying model is the same for each period; and for precipitation and hydrological sensitivity the outliers can be seen to show the same aerosol-driven pattern across the periods as the median response. The outliers are likely reflections of differing climate sensitivities in the models (Table 2). As shown in Figure 3e, there are large positive trends in both global mean temperature and precipitation, which contribute to the magnitude of the anomalies shown in Figure 6. Models in Figure 6 with large temperature anomalies are CanESM5 and UKESM1-0-LL. MIROC6 has the smallest anomalies. These models are also those with the highest and lowest equilibrium climate sensitivities in our ensemble (Table 2). For precipitation, the large outlier is UKESM1-0-LL and the small outlier is CAMS-CSM1-0. The precipitation climatologies and future changes for these models can be seen in Supplementary Figures 1-5, and 9.

4 Asian summer monsoon response

The decrease in Asian monsoon precipitation observed in the second half of the twentieth century has been largely attributed to the global increase in anthropogenic aerosols (Bollasina et al. (2011); Song et al. (2014); Polson et al. (2014)). The hemispheric asymmetry in aerosol forcing leads to an energy imbalance between the hemispheres, which in turn causes a slowdown of the meridional overturning circulation, and a weakening of the monsoon circulation (Bollasina et al. (2011); Song et al. (2014); Lau and Kim (2017); Undorf et al. (2018)). Local aerosol emissions further modify monsoon circulation and precipitation (Cowan and Cai (2011); Guo et al. (2015); Undorf et al. (2018)). In contrast to anthropogenic aerosols, where circulation changes are an important component of the response to forcing, GHGs mainly affect (increase) monsoon precipitation by enhancing tropospheric water vapour, and thus increasing moisture transport toward India (Li et al., 2015).

Global aerosol reductions in SSP1-1.9 briefly cause ~~this scenario to warm faster than the others consideredover Asia and East Asia~~faster warming over all Asian regions than the other scenarios considered, but this effect does not persist beyond the ~~2030s, and is not apparent over South Asia~~ 2040s (Figure 7a). However, anthropogenic aerosol does affect the regional pattern of warming (Figure 8), with slower increases in land temperature in many areas~~in~~ , and India in particular, in SSP2-4.5, 3-7.0, and 5-8.5 compared to SSP1-1.9. The growing influence of GHGs with time can also be seen in Figure 7a and 8 as greater warming in SSP5-8.5 compared to SSP2-4.5 ~~over the ocean, and over land from 2040.~~ in the 2040s. Continued increases in anthropogenic aerosol emissions in SSP3-7.0 appear to moderate land warming compared to other SSPs, despite large GHG increases (Figures 7a and 8).

~~As for the global mean case (Figure 6), the~~ The influence of aerosol is more clearly seen in regional mean precipitation than regional mean temperature (Figure 7~~b~~a, b; Figure 2), as for the global mean case (Figure 6b). Over Asia, the largest mean precipitation increase ~~occurs, for all decades,~~ relative to 1980-2014 occurs in SSP1-1.9 ~~, the smallest increases~~ for 2025-2034 and 2035-2044. The smallest precipitation increases are seen in SSP3-7.0 ~~, and comparable changes~~ during these periods. Increases in SSP2-4.5 ~~and SSP5-8.5~~lie between those in SSP3-7.0 and SSP1-1.9. The same pattern is ~~found~~ seen over East Asia~~for 2035-2044, but the picture is less clear for the other periods. This result could be a reflection of the role of internal variability or the transition to a period where precipitation increases are dominated by GHG changes, with East Asia warmer~~

relative to present day in SSP2-4.5 and . There is some indication that precipitation anomalies relative to 1980-2014 are slightly larger in SSP5-8.5 compared to SSP1-1.9by the 2050s (Figure 7a, Figure 8SSP2-4.5, but the growing difference between the two scenarios that was seen for temperature is not seen here. By 2100, GHGs are the dominant influence on the relative magnitude of the future increases in Asian summer monsoon precipitation across the SSPs, but the timing of the transition is model-dependent, as illustrated in Figure 9.

The pattern of the precipitation anomalies Over Asia and East Asia, precipitation increases relative to 1980-2014 across the SSPs is very different over South Asia compared to East Asia and Asia as a whole are significantly smaller in SSP3-7.0 compared to SSP1-1.9 until the mid-21st century (Figure 7). SSP1-1.9 and b). Over East Asia, JJA mean precipitation is not significantly larger than in 1980-2014 in SSP3-7.0 both result in increases in precipitation relative to the present day, while precipitation changes are small in SSP2-4.5 and 5-8.5, especially in prior to the 2050s. The effect of increased GHGs starts to become apparent by 2050, when larger precipitation increases are seen in SSP5-8.5 compared to SSP2-4.5 until 2045-2054. A similar pattern of aerosol-dominated differences between the SSPs is seen in hydrological sensitivity over Asia and East Asia (Figure 7), consistent with the temperature response (Figure 8).

The AOD anomaly compared to 1980-2014 in SSP2-4.5 is characterised by a dipole between increases in South Asian AOD and decreases c; Figure 2). The beginnings of the GHG influence are seen in hydrological sensitivity over East Asia . This pattern is present in observations since 2010 (Samset et al., 2019), and is in contrast to the twentieth century increases in both regions. The relatively small South Asian precipitation increases seen in SSP2-4.5 and in 2045-2054, when the SSP5-8.5 compared to SSP1-1.9 and SSP3-7.0, are likely to be due to suppressed warming over India due to continued anthropogenic aerosol increases there (Figure 1, 8). There is potential for this suppression to be enhanced by feedback between the East and South Asian monsoon system responses to forcing (Ha et al. (2018); Singh et al. (2019b))anomaly is slightly larger than that from SSP2-4.5. However, the clear GHG-dominated pattern seen for temperature is not seen here.

Figures 10 and 11 show that the pattern of Asian precipitation changes are similar, regardless of the emission pathway that is followed, but that the magnitude of the changes are pathway dependent, as summarised in Figure 7. Figure 10 shows the absolute anomaly compared to 1980-2014, while Figure 11 shows the anomaly relative to the SSP1-1.9 response. In Figure 11, the influence of GHGs can be seen, with greater GHG emissions driving greater drying over the Equatorial Indian Ocean and further increases in precipitation over India (particularly in the comparison between SSP2-4.5 and SSP5-8.5, and in SSP3-7.0 in the 2050s), as for temperature (Figure 8). Precipitation increases are smaller in SSP2-4.5, SSP3-7.0, and SSP5-8.5 compared to SSP1-1.9 (Figure 7, 10), mainly due to differences over northern India, Bangladesh, and the Bay of Bengal (Figure 11).

The pattern of precipitation anomalies relative to 1980-2014 across the SSPs is different over South Asia compared to East Asia and Asia (Figure 7). This suggests that the continued increases in local aerosol emissions may be relatively more important here than the remote decreases. All precipitation anomalies are positive, although many are not significantly different to zero. In 2025-2034 and 2035-2044 precipitation and hydrological sensitivity anomalies in SSP2-4.5 and SSP5-8.5 are smaller than those in SSP1-1.9 and SSP3-7.0, following neither the pattern expected from global and East Asian aerosol pathways, nor the GHG pathways. This similarity between SSP2-4.5 and SSP5-8.5, which is seen in all three periods for South Asia, suggests that the dipole in AOD anomalies between East Asia and South Asia in these scenarios (Figure 5) may be further suppressing

future increases in precipitation over South Asia due to feedback between the East and South Asian monsoon system responses to forcing (Ha et al. (2018); Singh et al. (2019b)). Overall, there is much more uncertainty in the South Asian precipitation changes compared to East Asia, as evidenced by the larger inter-model spread (Figure 7). Land use changes may also contribute to scenario uncertainty in South Asian precipitation changes (Singh et al., 2019a).

4.1 Aerosol only SSP2-4.5

Analysis of SSP2-4.5-aer, in which only anthropogenic aerosol emissions are varying with time following the SSP2-4.5 pathway, allows the response to aerosol changes to be isolated from that due to GHG~~changes~~. In this case, a dipole in temperature anomalies, with cooling over India and warming over East Asia, and in ~~sea level~~ sea-level pressure, with a positive anomaly over India, the Bay of Bengal, and the ~~Indo-China~~ Indochina peninsula, and a negative anomaly over the rest of Asia, can clearly be seen in both ~~CanESM5~~ MIROC6 (Figure 12) and ~~MIROC6~~ CanESM5 (Figure S7). This feature matches the dipole pattern in AOD changes (Figure 5), and is apparent in the SSP2-4.5 response up to 2050 as a moderated GHG-induced warming over South Asian relative to East Asia (Figure 8~~).~~ , Figure 13). Comparing the SSP2-4.5aer and SSP2-4.5 responses (Figure 12 vs. Figure 13 for MIROC6; Figure S7 vs. S8 for CanESM5) shows that aerosol largely acts to offset the GHG-driven response, rather than determining the overall pattern of the response.

Differences in the character of the precipitation anomaly can be seen when comparing the anomalies pre- and post-2050. In the earlier ~~periods~~period, when South Asian aerosol emissions continue to increase, precipitation anomalies are either weakly positive or negative over India, the Bay of Bengal, and the ~~Indo-China~~ Indochina peninsula. Post-2050, when anthropogenic aerosols are decreasing throughout Asia, precipitation increases are larger relative to 1980-2014. There are also suggestions of this structure in the CMIP6 mean SSP2-4.5 response, where increases in precipitation are weak over India and the Bay of Bengal compared to the SSP1-1.9 response (Figure 10, 11), but it is not as clear. This is likely partly due to the influence of GHG increases, and partly due to the effects of taking the mean response over models with large differences in their mean precipitation field (Figure 4~~;~~). However, a number of the individual models do simulate a similar tripolar pattern in precipitation change in SSP2-4. 5 ~~(Figure S8))~~to those in MIROC6 (Figure 10; Figure 11; Figure S9).

5 Conclusions

There is large uncertainty in future anthropogenic aerosol emission pathways. This is likely to be of limited importance for global-mean temperature, but anthropogenic aerosol does play an important role in changes in regional temperature ~~,~~and global and regional precipitation until 2050 under the Shared Socioeconomic Pathways. Rapid reductions in anthropogenic aerosol and precursor emissions in SSP1-1.9 lead to larger increases in global and Asian summer monsoon precipitation compared to SSP2-4.5, 3-7.0, and 5-8.5 over East Asia and ~~especially South Asia~~South Asia, despite the large decrease in greenhouse gases in SSP1-1.9.

In SSP2-4.5~~anthropogenic aerosol continues to increase~~ , 3.-7.0, and 5-8.5, anthropogenic aerosol emissions continue to increase until the mid-21st century over South Asia~~, in contrast to decreases over East Asia~~. This leads to ~~a suppressed~~

precipitation increase over South Asia in weaker future increases in regional precipitation until 2050, compared to SSP1-1.9, particularly over northern India. In SSP2-4.5 over the next 30 years in this scenario relative and 5-8.5 continued increases in South Asian aerosol optical depth occur while it decreases over East Asia. This may further suppress the precipitation increases in northern India compared to SSP1-1.9and SSP3-7.0. Such a . However, there is large inter-model uncertainty in the South Asian precipitation changes.

A dipole in aerosol optical depth trends over Asia has been observed over Asia since 2010 (Samset et al., 2019), suggesting that SSP2-4.5, SSP5-8.5 (where the current pattern persists), or SSP1-1.9 (where anthropogenic aerosol is reduced in both regions), are more likely to be followed in the real world than SSP3-7.0 (where anthropogenic aerosol increases in both regions). This presents the possibility of large uncertainty in South Asian summer monsoon precipitation on a 30-50 year time horizon due to uncertainty in local aerosol emission pathways.

Data availability. All data used in this work are freely available for research purposes.

Author contributions. All authors designed the analysis and wrote the paper. LJW, ZL, BHS, EH, MTL, KN, and SU performed the analysis.

Competing interests. The authors declare that they have no conflict of interest.

Acknowledgements. This work and its contributors Laura Wilcox, Zhen Liu, and Massimo Bollasina were supported by the UK-China Research & Innovation Partnership Fund through the Met Office Climate Science for Service Partnership (CSSP) China as part of the Newton Fund. Laura Wilcox received additional support from the Natural Environment Research Council (NERC; grant NE/S004890/1) and the International Meteorological Institute (IMI) visiting scientist program. Kalle Nordling and Joonas Merikanto acknowledge support from the Academy of Finland project RECIA (grant no. 287440) and European Research Council project ECLAIR (grant no. 646857).

We acknowledge the World Climate Research Programme, which, through its Working Group on Coupled Modelling, coordinated and promoted CMIP6. We thank the climate modelling groups for producing and making available their model output, the Earth System Grid Federation (ESGF) for archiving the data and providing access, and the multiple funding agencies who support CMIP6 and ESGF. APHRODITE precipitation data are available from http://www.chikyu.ac.jp/precip. GISTEMP temperature data, and CMAP, GPCC, and GPCP precipitation data were provided by the NOAA/OAR/ESRL PSD, Boulder, Colorado, USA, from their website at https://www.esrl.noaa.gov/psd/. We also acknowledge the use of ERA-Interim data produced by ECMWF and provided by the British Atmospheric Data Centre and the National Centre for Atmospheric Science. The analysis in this work was performed on the JASMIN super-data-cluster (Lawrence et al., 2012). JASMIN is managed and delivered by the UK Science and Technology Facilities Council (STFC) Centre for Environmental Data Archival (CEDA).

References

Acosta Navarro, J. C., Varma, V., Riipinen, I., Seland, Ø., Kirkevåg, A., Struthers, H., Iversen, T., Hansson, H. C., and Ekman, A. M. L.: Amplification of Arctic warming by past air pollution reductions in Europe, Nature Geoscience, 9, http://dx.doi.org/10.1038/ngeo2673, 2016.

Acosta Navarro, J. C., Ekman, A. M. L., Pausata, F. S. R., Lewinschal, A., Varma, V., Seland, Ø., Gauss, M., Iversen, T., Kirkevåg, A., Riipinen, I., Hansson, H. C., Navarro, J. C. A., Ekman, A. M. L., Pausata, F. S. R., Lewinschal, A., Varma, V., Seland, Ø., Gauss, M., Iversen, T., Kirkevåg, A., Riipinen, I., and Hansson, H. C.: Future Response of Temperature and Precipitation to Reduced Aerosol Emissions as Compared with Increased Greenhouse Gas Concentrations, Journal of Climate, 30, 939–954, https://doi.org/10.1175/JCLI-D-16-0466.1, http://journals.ametsoc.org/doi/10.1175/JCLI-D-16-0466.1, 2017.

Adler, R. F., Huffman, G. J., Chang, A., Ferraro, R., Xie, P.-P., Janowiak, J., Rudolf, B., Schneider, U., Curtis, S., Bolvin, D., Gruber, A., Susskind, J., Arkin, P., Nelkin, E., Adler, R. F., Huffman, G. J., Chang, A., Ferraro, R., Xie, P.-P., Janowiak, J., Rudolf, B., Schneider, U., Curtis, S., Bolvin, D., Gruber, A., Susskind, J., Arkin, P., and Nelkin, E.: The Version-2 Global Precipitation Climatology Project (GPCP) Monthly Precipitation Analysis (1979–Present), Journal of Hydrometeorology, 4, 1147–1167, https://doi.org/10.1175/1525-7541(2003)004<1147:TVGPCP>2.0.CO;2, http://journals.ametsoc.org/doi/abs/10.1175/1525-7541{%}282003{%}29004{%}3C1147{%}3ATVGPCP{%}3E2.0.CO{%}3B2, 2003.

Andrews, T.: MOHC HadGEM3-GC31-LL model output prepared for CMIP6 RFMIP, https://doi.org/10.22033/ESGF/CMIP6.475, https://doi.org/10.22033/ESGF/CMIP6.475, 2019.

Andrews, T., Forster, P. M., Boucher, O., Bellouin, N., and Jones, A.: Precipitation, radiative forcing and global temperature change, Geophysical Research Letters, 37, n/a–n/a, https://doi.org/10.1029/2010GL043991, http://doi.wiley.com/10.1029/2010GL043991, 2010.

Bartlett, R. E., Bollasina, M. A., Booth, B. B. B., Dunstone, N. J., Marenco, F., Messori, G., and Bernie, D. J.: Do differences in future sulfate emission pathways matter for near-term climate? A case study for the Asian monsoon, Climate Dynamics, 50, 1863–1880, https://doi.org/10.1007/s00382-017-3726-6, http://link.springer.com/10.1007/s00382-017-3726-6, 2018.

Bellouin, N., Rae, J., Jones, A., Johnson, C., Haywood, J., and Boucher, O.: Aerosol forcing in the Climate Model Intercomparison Project (CMIP5) simulations by HadGEM2-ES and the role of ammonium nitrate, Journal of Geophysical Research, 116, D20 206, https://doi.org/10.1029/2011JD016074, http://doi.wiley.com/10.1029/2011JD016074, 2011.

Bellouin, N., Mann, G. W., Woodhouse, M. T., Johnson, C., Carslaw, K. S., and Dalvi, M.: Impact of the modal aerosol scheme GLOMAP-mode on aerosol forcing in the Hadley Centre Global Environmental Model, Atmospheric Chemistry and Physics, 13, 3027–3044, https://doi.org/10.5194/acp-13-3027-2013, https://www.atmos-chem-phys.net/13/3027/2013/, 2013.

Bellouin, N., Quaas, J., Gryspeerdt, E., Kinne, S., Stier, P., Watson Parris, D., Boucher, O., Carslaw, K., Christensen, M., Daniau, A., Dufresne, J., Feingold, G., Fiedler, S., Forster, P., Gettelman, A., Haywood, J., Lohmann, U., Malavelle, F., Mauritsen, T., McCoy, D., Myhre, G., Mülmenstädt, J., Neubauer, D., Possner, A., Rugenstein, M., Sato, Y., Schulz, M., Schwartz, S., Sourdeval, O., Storelvmo, T., Toll, V., Winker, D., and Stevens, B.: Bounding global aerosol radiative forcing of climate change, Reviews of Geophysics, p. 2019RG000660, https://doi.org/10.1029/2019RG000660, https://onlinelibrary.wiley.com/doi/abs/10.1029/2019RG000660, 2019.

Bollasina, M. A., Ming, Y., and Ramaswamy, V.: Anthropogenic aerosols and the weakening of the South Asian summer monsoon., Science (New York, N.Y.), 334, 502–5, https://doi.org/10.1126/science.1204994, http://www.ncbi.nlm.nih.gov/pubmed/21960529, 2011.

Boucher, O., Randall, D., Artaxo, P., Bretherton, C., Feingold, G., Forster, P., Kerminen, V.-M., Kondo, Y., Liao, H., Lohmann, U., Rasch, P., Satheesh, S., Sherwood, S., Stevens, B., and Zhang, X.-Y.: Clouds and Aerosols. In: Climate Change 2013: The Physical Science Basis.

Contribution of Working Group I to the Fifth Assessment Report of the Intergovernmental Panel on Climate Change, Climate Change 2013: The Physical Science Basis. Contribution of Working Group I to the Fifth Assessment Report of the Intergovernmental Panel on Climate Change, 2013.

Boucher, O., Denvil, S., Caubel, A., and Foujols, M. A.: IPSL IPSL-CM6A-LR model output prepared for CMIP6 CMIP historical, https://doi.org/10.22033/ESGF/CMIP6.5195, https://doi.org/10.22033/ESGF/CMIP6.5195, 2018a.

Boucher, O., Denvil, S., Caubel, A., and Foujols, M. A.: IPSL IPSL-CM6A-LR model output prepared for CMIP6 RFMIP, https://doi.org/10.22033/ESGF/CMIP6.1531, https://doi.org/10.22033/ESGF/CMIP6.1531, 2018b.

Boucher, O., Denvil, S., Caubel, A., and Foujols, M. A.: IPSL IPSL-CM6A-LR model output prepared for CMIP6 ScenarioMIP, https://doi.org/10.22033/ESGF/CMIP6.1532, https://doi.org/10.22033/ESGF/CMIP6.1532, 2019.

Chalmers, N., Highwood, E. J., Hawkins, E., Sutton, R., and Wilcox, L. J.: Aerosol contribution to the rapid warming of near-term climate under RCP 2.6, Geophysical Research Letters, 39, https://doi.org/10.1029/2012GL052848, http://doi.wiley.com/10.1029/2012GL052848, 2012.

Collins, M., AchutaRao, K., Ashok, K., Bhandari, S., Mitra, A. K., Prakash, S., Srivastava, R., and Turner, A.: Observational challenges in evaluating climate models, Nature Climate Change, 3, 940–941, https://doi.org/10.1038/nclimate2012, http://www.nature.com/articles/nclimate2012, 2013.

Cowan, T. and Cai, W.: The impact of Asian and non-Asian anthropogenic aerosols on 20th century Asian summer monsoon, Geophysical Research Letters, 38, n/a–n/a, https://doi.org/10.1029/2011GL047268, http://doi.wiley.com/10.1029/2011GL047268, 2011.

Danabasoglu, G.: NCAR CESM2 model output prepared for CMIP6 CMIP historical, https://doi.org/10.22033/ESGF/CMIP6.7627, https://doi.org/10.22033/ESGF/CMIP6.7627, 2019a.

Danabasoglu, G.: NCAR CESM2 model output prepared for CMIP6 RFMIP, https://doi.org/10.22033/ESGF/CMIP6.2199, https://doi.org/10.22033/ESGF/CMIP6.2199, 2019b.

Dee, D. P., Uppala, S. M., Simmons, A. J., Berrisford, P., Poli, P., Kobayashi, S., Andrae, U., Balmaseda, M. A., Balsamo, G., Bauer, P., Bechtold, P., Beljaars, A. C. M., van de Berg, L., Bidlot, J., Bormann, N., Delsol, C., Dragani, R., Fuentes, M., Geer, A. J., Haimberger, L., Healy, S. B., Hersbach, H., Hólm, E. V., Isaksen, L., Kållberg, P., Köhler, M., Matricardi, M., McNally, A. P., Monge-Sanz, B. M., Morcrette, J.-J., Park, B.-K., Peubey, C., de Rosnay, P., Tavolato, C., Thépaut, J.-N., and Vitart, F.: The ERA-Interim reanalysis: configuration and performance of the data assimilation system, Quarterly Journal of the Royal Meteorological Society, 137, 553–597, https://doi.org/10.1002/qj.828, http://doi.wiley.com/10.1002/qj.828, 2011.

Dong, B., Sutton, R., Highwood, E., and Wilcox, L.: Preferred response of the East Asian summer monsoon to local and non-local anthropogenic sulphur dioxide emissions, Climate Dynamics, 46, https://doi.org/10.1007/s00382-015-2671-5, 2016.

(EC-Earth), E.-E. C.: EC-Earth-Consortium EC-Earth3-Veg model output prepared for CMIP6 CMIP historical, https://doi.org/10.22033/ESGF/CMIP6.4706, https://doi.org/10.22033/ESGF/CMIP6.4706, 2019a.

(EC-Earth), E.-E. C.: EC-Earth-Consortium EC-Earth3-Veg model output prepared for CMIP6 ScenarioMIP, https://doi.org/10.22033/ESGF/CMIP6.727, https://doi.org/10.22033/ESGF/CMIP6.727, 2019b.

Eyring, V., Bony, S., Meehl, G. A., Senior, C. A., Stevens, B., Stouffer, R. J., and Taylor, K. E.: Overview of the Coupled Model Intercomparison Project Phase 6 (CMIP6) experimental design and organization, Geoscientific Model Development, 9, 1937–1958, https://doi.org/10.5194/gmd-9-1937-2016, https://www.geosci-model-dev.net/9/1937/2016/, 2016.

Fläschner, D., Mauritsen, T., Stevens, B., Fläschner, D., Mauritsen, T., and Stevens, B.: Understanding the Intermodel Spread in Global-Mean Hydrological Sensitivity, Journal of Climate, 29, 801–817, https://doi.org/10.1175/JCLI-D-15-0351.1, http://journals.ametsoc.org/doi/10.1175/JCLI-D-15-0351.1, 2016.

for Space Studies (NASA/GISS), N. G. I.: NASA-GISS GISS-E2.1G model output prepared for CMIP6 CMIP historical, https://doi.org/10.22033/ESGF/CMIP6.7127, https://doi.org/10.22033/ESGF/CMIP6.7127, 2018.

for Space Studies (NASA/GISS), N. G. I.: NASA-GISS GISS-E2.1G model output prepared for CMIP6 RFMIP, https://doi.org/10.22033/ESGF/CMIP6.2072, https://doi.org/10.22033/ESGF/CMIP6.2072, 2019.

Gillett, N. P. and Von Salzen, K.: The role of reduced aerosol precursor emissions in driving near-term warming, Environmental Research Letters, 8, 034 008, https://doi.org/10.1088/1748-9326/8/3/034008, http://stacks.iop.org/1748-9326/8/i=3/a=034008?key=crossref.5e0362958468b043159465bd9c0f913d, 2013.

Gillett, N. P., Shiogama, H., Funke, B., Hegerl, G., Knutti, R., Matthes, K., Santer, B. D., Stone, D., and Tebaldi, C.: The Detection and Attribution Model Intercomparison Project (DAMIP v1.0) contribution to CMIP6, Geoscientific Model Development, 9, 3685–3697, https://doi.org/10.5194/gmd-9-3685-2016, https://www.geosci-model-dev.net/9/3685/2016/, 2016.

Good, P., Sellar, A., Tang, Y., Rumbold, S., Ellis, R., Kelley, D., Kuhlbrodt, T., and Walton, J.: MOHC UKESM1.0-LL model output prepared for CMIP6 ScenarioMIP, https://doi.org/10.22033/ESGF/CMIP6.1567, https://doi.org/10.22033/ESGF/CMIP6.1567, 2019.

Guo, H., John, J. G., Blanton, C., McHugh, C., Nikonov, S., Radhakrishnan, A., Zadeh, N. T., Balaji, V., Durachta, J., Dupuis, C., Menzel, R., Robinson, T., Underwood, S., Vahlenkamp, H., Dunne, K. A., Gauthier, P. P., Ginoux, P., Griffies, S. M., Hallberg, R., Harrison, M., Hurlin, W., Lin, P., Malyshev, S., Naik, V., Paulot, F., Paynter, D. J., Ploshay, J., Schwarzkopf, D. M., Seman, C. J., Shao, A., Silvers, L., Wyman, B., Yan, X., Zeng, Y., Adcroft, A., Dunne, J. P., Held, I. M., Krasting, J. P., Horowitz, L. W., Milly, C., Shevliakova, E., Winton, M., Zhao, M., and Zhang, R.: NOAA-GFDL GFDL-CM4 model output prepared for CMIP6 ScenarioMIP, https://doi.org/10.22033/ESGF/CMIP6.9242, https://doi.org/10.22033/ESGF/CMIP6.9242, 2018a.

Guo, H., John, J. G., Blanton, C., McHugh, C., Nikonov, S., Radhakrishnan, A., Zadeh, N. T., Balaji, V., Durachta, J., Dupuis, C., Menzel, R., Robinson, T., Underwood, S., Vahlenkamp, H., Dunne, K. A., Gauthier, P. P., Ginoux, P., Griffies, S. M., Hallberg, R., Harrison, M., Hurlin, W., Malyshev, S., Naik, V., Paulot, F., Paynter, D. J., Ploshay, J., Schwarzkopf, D. M., Seman, C. J., Shao, A., Silvers, L., Wyman, B., Zeng, Y., Adcroft, A., Dunne, J. P., Held, I. M., Krasting, J. P., Horowitz, L. W., Milly, P., Shevliakova, E., Winton, M., and Zhao, M.: NOAA-GFDL GFDL-CM4 model output prepared for CMIP6 CMIP historical, https://doi.org/10.22033/ESGF/CMIP6.8594, https://doi.org/10.22033/ESGF/CMIP6.8594, 2018b.

Guo, L., Turner, A. G., and Highwood, E. J.: Impacts of 20th century aerosol emissions on the South Asian monsoon in the CMIP5 models, Atmospheric Chemistry and Physics, 15, 6367–6378, https://doi.org/10.5194/acp-15-6367-2015, https://www.atmos-chem-phys.net/15/6367/2015/, 2015.

Guo, L., Turner, A. G., Highwood, E. J., Guo, L., Turner, A. G., and Highwood, E. J.: Local and Remote Impacts of Aerosol Species on Indian Summer Monsoon Rainfall in a GCM, Journal of Climate, 29, 6937–6955, https://doi.org/10.1175/JCLI-D-15-0728.1, http://journals.ametsoc.org/doi/10.1175/JCLI-D-15-0728.1, 2016.

Gusain, A., Ghosh, S., and Karmakar, S.: Added value of CMIP6 over CMIP5 models in simulating Indian summer monsoon rainfall, Atmospheric Research, 232, 104 680, https://doi.org/10.1016/J.ATMOSRES.2019.104680, https://www.sciencedirect.com/science/article/pii/S0169809519307665{#}coi0005, 2020.

Ha, K.-J., Seo, Y.-W., Lee, J.-Y., Kripalani, R. H., and Yun, K.-S.: Linkages between the South and East Asian summer monsoons: a review and revisit, Climate Dynamics, 51, 4207–4227, https://doi.org/10.1007/s00382-017-3773-z, http://link.springer.com/10.1007/s00382-017-3773-z, 2018.

Hansen, J., Ruedy, R., Sato, M., and Lo, K.: Global surface temperature change, Reviews of Geophysics, 48, RG4004, https://doi.org/10.1029/2010RG000345, http://doi.wiley.com/10.1029/2010RG000345, 2010.

Hegerl, G. C., Brönnimann, S., Cowan, T., Friedman, A. R., Hawkins, E., Iles, C., Müller, W., Schurer, A., and Undorf, S.: Causes of climate change over the historical record, Environmental Research Letters, 14, 123 006, https://doi.org/10.1088/1748-9326/ab4557, https://iopscience.iop.org/article/10.1088/1748-9326/ab4557, 2019.

Hienola, A., Partanen, A.-I., Pietikäinen, J.-P., O'Donnell, D., Korhonen, H., Matthews, H. D., and Laaksonen, A.: The impact of aerosol emissions on the 1.5 °C pathways, Environmental Research Letters, 13, 044 011, https://doi.org/10.1088/1748-9326/aab1b2, http://stacks.iop.org/1748-9326/13/i=4/a=044011?key=crossref.038a7a508aa27527067e48e972e2db8e, 2018.

Huang, B., Thorne, P. W., Banzon, V. F., Boyer, T., Chepurin, G., Lawrimore, J. H., Menne, M. J., Smith, T. M., Vose, R. S., and Zhang, H.-M.: Extended Reconstructed Sea Surface Temperature, Version 5 (ERSSTv5): Upgrades, Validations, and Intercomparisons, Journal of Climate, 30, 8179–8205, https://doi.org/10.1175/JCLI-D-16-0836.1, http://journals.ametsoc.org/doi/10.1175/JCLI-D-16-0836.1, 2017.

Jones, G. S., Stott, P. A., and Christidis, N.: Attribution of observed historical near-surface temperature variations to anthropogenic and natural causes using CMIP5 simulations, Journal of Geophysical Research: Atmospheres, 118, 4001–4024, https://doi.org/10.1002/jgrd.50239, http://doi.wiley.com/10.1002/jgrd.50239, 2013.

Kirkevåg, A., Grini, A., Olivié, D., Seland, Ø., Alterskjær, K., Hummel, M., Karset, I. H. H., Lewinschal, A., Liu, X., Makkonen, R., Bethke, I., Griesfeller, J., Schulz, M., and Iversen, T.: A production-tagged aerosol module for Earth system models, OsloAero5.3 – extensions and updates for CAM5.3-Oslo, Geoscientific Model Development, 11, 3945–3982, https://doi.org/10.5194/gmd-11-3945-2018, https://www.geosci-model-dev.net/11/3945/2018/, 2018.

Klimont, Z., Kupiainen, K., Heyes, C., Purohit, P., Cofala, J., Rafaj, P., Borken-Kleefeld, J., and Schöpp, W.: Global anthropogenic emissions of particulate matter including black carbon, Atmospheric Chemistry and Physics, 17, 8681–8723, https://doi.org/10.5194/acp-17-8681-2017, https://www.atmos-chem-phys.net/17/8681/2017/, 2017.

Kloster, S., Dentener, F., Feichter, J., Raes, F., Lohmann, U., Roeckner, E., and Fischer-Bruns, I.: A GCM study of future climate response to aerosol pollution reductions, Climate Dynamics, 34, 1177–1194, https://doi.org/10.1007/s00382-009-0573-0, http://link.springer.com/10.1007/s00382-009-0573-0, 2010.

Lau, W. K.-M. and Kim, K.-M.: Competing influences of greenhouse warming and aerosols on Asian summer monsoon circulation and rainfall, Asia-Pacific Journal of Atmospheric Sciences, 53, 181–194, https://doi.org/10.1007/s13143-017-0033-4, http://link.springer.com/10.1007/s13143-017-0033-4, 2017.

Lawrence, B., Bennett, V. L., Churchill, J., Juckes, M., Kershaw, P., Oliver, P., Pritchard, M., and Stephens, A.: The JASMIN super-data-cluster, arXiv preprint arXiv:1204.3553, https://www.academia.edu/2871931/The{_}JASMIN{_}super-data-cluster, 2012.

Lenssen, N. J. L., Schmidt, G. A., Hansen, J. E., Menne, M. J., Persin, A., Ruedy, R., and Zyss, D.: Improvements in the GISTEMP Uncertainty Model, Journal of Geophysical Research: Atmospheres, 124, 6307–6326, https://doi.org/10.1029/2018JD029522, https://onlinelibrary.wiley.com/doi/abs/10.1029/2018JD029522, 2019.

Levy, H., Horowitz, L. W., Schwarzkopf, M. D., Ming, Y., Golaz, J.-C., Naik, V., and Ramaswamy, V.: The roles of aerosol direct and indirect effects in past and future climate change, Journal of Geophysical Research: Atmospheres, 118, 4521–4532, https://doi.org/10.1002/jgrd.50192, http://doi.wiley.com/10.1002/jgrd.50192, 2013.

Li, X., Ting, M., Li, C., Henderson, N., Li, X., Ting, M., Li, C., and Henderson, N.: Mechanisms of Asian Summer Monsoon Changes in Response to Anthropogenic Forcing in CMIP5 Models, Journal of Climate, 28, 4107–4125, https://doi.org/10.1175/JCLI-D-14-00559.1, http://journals.ametsoc.org/doi/10.1175/JCLI-D-14-00559.1, 2015.

Liepert, B. G., Feichter, J., Lohmann, U., and Roeckner, E.: Can aerosols spin down the water cycle in a warmer and moister world?, Geophysical Research Letters, 31, n/a–n/a, https://doi.org/10.1029/2003GL019060, http://doi.wiley.com/10.1029/2003GL019060, 2004.

Liepert, B. G., Previdi, M., Liepert, B. G., and Previdi, M.: Do Models and Observations Disagree on the Rainfall Response to Global Warming?, Journal of Climate, 22, 3156–3166, https://doi.org/10.1175/2008JCLI2472.1, http://journals.ametsoc.org/doi/10.1175/2008JCLI2472.1, 2009.

Liu, L., Shawki, D., Voulgarakis, A., Kasoar, M., Samset, B. H., Myhre, G., Forster, P. M., Hodnebrog, Ø., Sillmann, J., Aalbergsjø, S. G., Boucher, O., Faluvegi, G., Iversen, T., Kirkevåg, A., Lamarque, J.-F., Olivié, D., Richardson, T., Shindell, D., Takemura, T., Liu, L., Shawki, D., Voulgarakis, A., Kasoar, M., Samset, B. H., Myhre, G., Forster, P. M., Hodnebrog, Ø., Sillmann, J., Aalbergsjø, S. G., Boucher, O., Faluvegi, G., Iversen, T., Kirkevåg, A., Lamarque, J.-F., Olivié, D., Richardson, T., Shindell, D., and Takemura, T.: A PDRMIP Multimodel Study on the Impacts of Regional Aerosol Forcings on Global and Regional Precipitation, Journal of Climate, 31, 4429–4447, https://doi.org/10.1175/JCLI-D-17-0439.1, http://journals.ametsoc.org/doi/10.1175/JCLI-D-17-0439.1, 2018.

Lund, M. T., Myhre, G., Haslerud, A. S., Skeie, R. B., Griesfeller, J., Platt, S. M., Kumar, R., Myhre, C. L., and Schulz, M.: Concentrations and radiative forcing of anthropogenic aerosols from 1750 to 2014 simulated with the Oslo CTM3 and CEDS emission inventory, Geoscientific Model Development, 11, 4909–4931, https://doi.org/10.5194/gmd-11-4909-2018, https://www.geosci-model-dev.net/11/4909/2018/, 2018.

McGill, R., Tukey, J. W., and Larsen, W. A.: Variations of box plots, American Statistician, 32, 12–16, https://doi.org/10.1080/00031305.1978.10479236, 1978.

Menne, M. J., Williams, C. N., Gleason, B. E., Rennie, J. J., and Lawrimore, J. H.: The Global Historical Climatology Network Monthly Temperature Dataset, Version 4, Journal of Climate, 31, 9835–9854, https://doi.org/10.1175/JCLI-D-18-0094.1, http://journals.ametsoc.org/doi/10.1175/JCLI-D-18-0094.1, 2018.

Moss, R. H., Edmonds, J. A., Hibbard, K. A., Manning, M. R., Rose, S. K., van Vuuren, D. P., Carter, T. R., Emori, S., Kainuma, M., Kram, T., Meehl, G. A., Mitchell, J. F. B., Nakicenovic, N., Riahi, K., Smith, S. J., Stouffer, R. J., Thomson, A. M., Weyant, J. P., and Wilbanks, T. J.: The next generation of scenarios for climate change research and assessment, Nature, 463, 747–756, https://doi.org/10.1038/nature08823, http://www.nature.com/articles/nature08823, 2010.

Mulcahy, J. P., Jones, C., Sellar, A., Johnson, B., Boutle, I. A., Jones, A., Andrews, T., Rumbold, S. T., Mollard, J., Bellouin, N., Johnson, C. E., Williams, K. D., Grosvenor, D. P., and McCoy, D. T.: Improved Aerosol Processes and Effective Radiative Forcing in HadGEM3 and UKESM1, Journal of Advances in Modeling Earth Systems, 10, 2786–2805, https://doi.org/10.1029/2018MS001464, https://onlinelibrary.wiley.com/doi/abs/10.1029/2018MS001464, 2018.

Nordling, K., Korhonen, H., Räisänen, P., Alper, M. E., Uotila, P., O'Donnell, D., and Merikanto, J.: Role of climate model dynamics in estimated climate responses to anthropogenic aerosols, Atmospheric Chemistry and Physics, 19, 9969–9987, https://doi.org/10.5194/acp-19-9969-2019, https://www.atmos-chem-phys.net/19/9969/2019/, 2019.

O'Connor, F., Dalvi, M., Kahana, R., Johnson, B., Mulcahy, J., Robertson, E., Shim, S., and Wiltshire, A.: MOHC UKESM1.0-LL model output prepared for CMIP6 RFMIP, https://doi.org/10.22033/ESGF/CMIP6.11061, https://doi.org/10.22033/ESGF/CMIP6.11061, 2019.

O'Neill, B. C., Tebaldi, C., van Vuuren, D. P., Eyring, V., Friedlingstein, P., Hurtt, G., Knutti, R., Kriegler, E., Lamarque, J.-F., Lowe, J., Meehl, G. A., Moss, R., Riahi, K., and Sanderson, B. M.: The Scenario Model Intercomparison Project (ScenarioMIP) for CMIP6,

Geoscientific Model Development, 9, 3461–3482, https://doi.org/10.5194/gmd-9-3461-2016, https://www.geosci-model-dev.net/9/3461/2016/, 2016.

Partanen, A.-I., Landry, J.-S., and Matthews, H. D.: Climate and health implications of future aerosol emission scenarios, Environmental Research Letters, 13, 024 028, https://doi.org/10.1088/1748-9326/aaa511, http://stacks.iop.org/1748-9326/13/i=2/a=024028?key=crossref.92c5bb2bc9b2717c4d48fe03d3ba8af8, 2018.

Paynter, D. J., Menzel, R., Jones, A., Schwarzkopf, D. M., Freidenreich, S., Wyman, B., Blanton, C., McHugh, C., Radhakrishnan, A., Vahlenkamp, H., Rand, K., Silvers, L., Guo, H., John, J. G., Ploshay, J., Balaji, V., and Wilson, C.: NOAA-GFDL GFDL-CM4 model output prepared for CMIP6 RFMIP, https://doi.org/10.22033/ESGF/CMIP6.1643, https://doi.org/10.22033/ESGF/CMIP6.1643, 2018.

Pendergrass, A. G.: apendergrass/cmip6-ecs: Initial release with DOI and data in CSV format, https://doi.org/10.5281/ZENODO.3492165, 2019.

Pietikäinen, J.-P., Kupiainen, K., Klimont, Z., Makkonen, R., Korhonen, H., Karinkanta, R., Hyvärinen, A.-P., Karvosenoja, N., Laaksonen, A., Lihavainen, H., and Kerminen, V.-M.: Impacts of emission reductions on aerosol radiative effects, Atmospheric Chemistry and Physics, 15, 5501–5519, https://doi.org/10.5194/acp-15-5501-2015, https://www.atmos-chem-phys.net/15/5501/2015/, 2015.

Platnick, S.: MODIS Atmosphere L3 Monthly Product, NASA MODIS Adaptive Processing System, https://doi.org/http://dx.doi.org/10.5067/MODIS/MYD08_M3.006, https://modaps.modaps.eosdis.nasa.gov/services/about/products/c6/MYD08{_}M3.html, 2015.

Polson, D., Bollasina, M., Hegerl, G. C., and Wilcox, L. J.: Decreased monsoon precipitation in the Northern Hemisphere due to anthropogenic aerosols, Geophysical Research Letters, 41, 6023–6029, https://doi.org/10.1002/2014GL060811, http://doi.wiley.com/10.1002/2014GL060811, 2014.

Prakash, S., Mitra, A. K., Momin, I. M., Rajagopal, E. N., Basu, S., Collins, M., Turner, A. G., Achuta Rao, K., and Ashok, K.: Seasonal intercomparison of observational rainfall datasets over India during the southwest monsoon season, International Journal of Climatology, 35, 2326–2338, https://doi.org/10.1002/joc.4129, http://doi.wiley.com/10.1002/joc.4129, 2015.

Rao, S., Klimont, Z., Smith, S. J., Van Dingenen, R., Dentener, F., Bouwman, L., Riahi, K., Amann, M., Bodirsky, B. L., van Vuuren, D. P., Aleluia Reis, L., Calvin, K., Drouet, L., Fricko, O., Fujimori, S., Gernaat, D., Havlik, P., Harmsen, M., Hasegawa, T., Heyes, C., Hilaire, J., Luderer, G., Masui, T., Stehfest, E., Strefler, J., van der Sluis, S., and Tavoni, M.: Future air pollution in the Shared Socio-economic Pathways, Global Environmental Change, 42, 346–358, https://doi.org/10.1016/J.GLOENVCHA.2016.05.012, https://www.sciencedirect.com/science/article/pii/S0959378016300723?via{%}3Dihub, 2017.

Remer, L. A., Kleidman, R. G., Levy, R. C., Kaufman, Y. J., Tanré, D., Mattoo, S., Martins, J. V., Ichoku, C., Koren, I., Yu, H., and Holben, B. N.: Global aerosol climatology from the MODIS satellite sensors, Journal of Geophysical Research, 113, D14S07, https://doi.org/10.1029/2007JD009661, http://doi.wiley.com/10.1029/2007JD009661, 2008.

Riahi, K., van Vuuren, D. P., Kriegler, E., Edmonds, J., O'Neill, B. C., Fujimori, S., Bauer, N., Calvin, K., Dellink, R., Fricko, O., Lutz, W., Popp, A., Cuaresma, J. C., KC, S., Leimbach, M., Jiang, L., Kram, T., Rao, S., Emmerling, J., Ebi, K., Hasegawa, T., Havlik, P., Humpenöder, F., Da Silva, L. A., Smith, S., Stehfest, E., Bosetti, V., Eom, J., Gernaat, D., Masui, T., Rogelj, J., Strefler, J., Drouet, L., Krey, V., Luderer, G., Harmsen, M., Takahashi, K., Baumstark, L., Doelman, J. C., Kainuma, M., Klimont, Z., Marangoni, G., Lotze-Campen, H., Obersteiner, M., Tabeau, A., and Tavoni, M.: The Shared Socioeconomic Pathways and their energy, land use, and greenhouse gas emissions implications: An overview, Global Environmental Change, 42, 153–168, https://doi.org/10.1016/J.GLOENVCHA.2016.05.009, https://www.sciencedirect.com/science/article/pii/S0959378016300681?via{%}3Dihub, 2017.

Ridley, J., Menary, M., Kuhlbrodt, T., Andrews, M., and Andrews, T.: MOHC HadGEM3-GC31-LL model output prepared for CMIP6 CMIP historical, https://doi.org/10.22033/ESGF/CMIP6.6109, https://doi.org/10.22033/ESGF/CMIP6.6109, 2019.

Rong, X.: CAMS CAMS CSM1.0 model output prepared for CMIP6 CMIP historical, https://doi.org/10.22033/ESGF/CMIP6.9754, https://doi.org/10.22033/ESGF/CMIP6.9754, 2019a.

Rong, X.: CAMS CAMS-CSM1.0 model output prepared for CMIP6 ScenarioMIP, https://doi.org/10.22033/ESGF/CMIP6.11004, https://doi.org/10.22033/ESGF/CMIP6.11004, 2019b.

Rotstayn, L. D., Collier, M. A., Chrastansky, A., Jeffrey, S. J., and Luo, J.-J.: Projected effects of declining aerosols in RCP4.5: unmasking global warming?, Atmospheric Chemistry and Physics, 13, 10 883–10 905, https://doi.org/10.5194/acp-13-10883-2013, https://www.atmos-chem-phys.net/13/10883/2013/, 2013.

Rotstayn, L. D., Collier, M. A., and Luo, J.-J.: Effects of declining aerosols on projections of zonally averaged tropical precipitation, Environmental Research Letters, 10, 044 018, https://doi.org/10.1088/1748-9326/10/4/044018, http://stacks.iop.org/1748-9326/10/i=4/a=044018?key=crossref.5295dd98eb7c1dc839889ae968219dad, 2015.

Salzmann, M.: Global warming without global mean precipitation increase?, Science Advances, 2, e1501 572, https://doi.org/10.1126/sciadv.1501572, http://advances.sciencemag.org/lookup/doi/10.1126/sciadv.1501572, 2016.

Samset, B. H., Myhre, G., Forster, P. M., Hodnebrog, Ø., Andrews, T., Faluvegi, G., Fläschner, D., Kasoar, M., Kharin, V., Kirkevåg, A., Lamarque, J., Olivié, D., Richardson, T., Shindell, D., Shine, K. P., Takemura, T., and Voulgarakis, A.: Fast and slow precipitation responses to individual climate forcers: A PDRMIP multimodel study, Geophysical Research Letters, 43, 2782–2791, https://doi.org/10.1002/2016GL068064, https://onlinelibrary.wiley.com/doi/abs/10.1002/2016GL068064, 2016.

Samset, B. H., Sand, M., Smith, C. J., Bauer, S. E., Forster, P. M., Fuglestvedt, J. S., Osprey, S., and Schleussner, C.-F.: Climate Impacts From a Removal of Anthropogenic Aerosol Emissions, Geophysical Research Letters, 45, 1020–1029, https://doi.org/10.1002/2017GL076079, http://doi.wiley.com/10.1002/2017GL076079, 2018.

Samset, B. H., Lund, M. T., Bollasina, M., Myhre, G., and Wilcox, L.: Emerging Asian aerosol patterns, Nature Geoscience, 12, 582–584, https://doi.org/10.1038/s41561-019-0424-5, http://www.nature.com/articles/s41561-019-0424-5, 2019.

Scannell, C., Booth, B. B. B., Dunstone, N. J., Rowell, D. P., Bernie, D. J., Kasoar, M., Voulgarakis, A., Wilcox, L. J., Acosta Navarro, J. C., Seland, Ø., and Paynter, D. J.: The Influence of Remote Aerosol Forcing from Industrialized Economies on the Future Evolution of East and West African Rainfall, Journal of Climate, 32, 8335–8354, https://doi.org/10.1175/JCLI-D-18-0716.1, http://journals.ametsoc.org/doi/10.1175/JCLI-D-18-0716.1, 2019.

Schneider, U., Becker, A., Finger, P., Meyer-Christoffer, A., Ziese, M., and Rudolf, B.: GPCC's new land surface precipitation climatology based on quality-controlled in situ data and its role in quantifying the global water cycle, Theoretical and Applied Climatology, 115, 15–40, https://doi.org/10.1007/s00704-013-0860-x, http://link.springer.com/10.1007/s00704-013-0860-x, 2014.

Seferian, R.: CNRM-CERFACS CNRM-ESM2-1 model output prepared for CMIP6 CMIP historical, https://doi.org/10.22033/ESGF/CMIP6.4068, https://doi.org/10.22033/ESGF/CMIP6.4068, 2018.

Seferian, R.: CNRM-CERFACS CNRM-ESM2-1 model output prepared for CMIP6 RFMIP, https://doi.org/10.22033/ESGF/CMIP6.9565, https://doi.org/10.22033/ESGF/CMIP6.9565, 2019a.

Seferian, R.: CNRM-CERFACS CNRM-ESM2-1 model output prepared for CMIP6 ScenarioMIP, https://doi.org/10.22033/ESGF/CMIP6.1395, https://doi.org/10.22033/ESGF/CMIP6.1395, 2019b.

Sekiguchi, M. and Shiogama, H.: MIROC MIROC6 model output prepared for CMIP6 RFMIP, https://doi.org/10.22033/ESGF/CMIP6.895, https://doi.org/10.22033/ESGF/CMIP6.895, 2019.

Shawki, D., Voulgarakis, A., Chakraborty, A., Kasoar, M., and Srinivasan, J.: The South Asian Monsoon Response to Remote Aerosols: Global and Regional Mechanisms, Journal of Geophysical Research: Atmospheres, 123, 11,585–11,601, https://doi.org/10.1029/2018JD028623, http://doi.wiley.com/10.1029/2018JD028623, 2018.

Shindell, D. and Smith, C. J.: Climate and air-quality benefits of a realistic phase-out of fossil fuels, Nature, 573, 408–411, https://doi.org/10.1038/s41586-019-1554-z, http://www.nature.com/articles/s41586-019-1554-z, 2019.

Shindell, D., Kuylenstierna, J. C. I., Vignati, E., van Dingenen, R., Amann, M., Klimont, Z., Anenberg, S. C., Muller, N., Janssens-Maenhout, G., Raes, F., Schwartz, J., Faluvegi, G., Pozzoli, L., Kupiainen, K., Höglund-Isaksson, L., Emberson, L., Streets, D., Ramanathan, V., Hicks, K., Oanh, N. T. K., Milly, G., Williams, M., Demkine, V., and Fowler, D.: Simultaneously mitigating near-term climate change and improving human health and food security., Science (New York, N.Y.), 335, 183–9, https://doi.org/10.1126/science.1210026, http://www.ncbi.nlm.nih.gov/pubmed/22246768, 2012.

Shiogama, H.: MIROC MIROC6 model output prepared for CMIP6 DAMIP, https://doi.org/10.22033/ESGF/CMIP6.894, https://doi.org/10.22033/ESGF/CMIP6.894, 2019.

Sillmann, J., Pozzoli, L., Vignati, E., Kloster, S., and Feichter, J.: Aerosol effect on climate extremes in Europe under different future scenarios, Geophysical Research Letters, 40, 2290–2295, https://doi.org/10.1002/grl.50459, http://doi.wiley.com/10.1002/grl.50459, 2013.

Singh, D., Bollasina, M., Ting, M., and Diffenbaugh, N. S.: Disentangling the influence of local and remote anthropogenic aerosols on South Asian monsoon daily rainfall characteristics, Climate Dynamics, 52, 6301–6320, https://doi.org/10.1007/s00382-018-4512-9, http://link.springer.com/10.1007/s00382-018-4512-9, 2019a.

Singh, D., Ghosh, S., Roxy, M. K., and McDermid, S.: Indian summer monsoon: Extreme events, historical changes, and role of anthropogenic forcings, Wiley Interdisciplinary Reviews: Climate Change, 10, https://doi.org/10.1002/wcc.571, https://onlinelibrary.wiley.com/doi/abs/10.1002/wcc.571, 2019b.

Smith, C. J., Forster, P. M., Allen, M., Leach, N., Millar, R. J., Passerello, G. A., and Regayre, L. A.: FAIR v1.3: a simple emissions-based impulse response and carbon cycle model, Geoscientific Model Development, 11, 2273–2297, https://doi.org/10.5194/gmd-11-2273-2018, https://www.geosci-model-dev.net/11/2273/2018/, 2018.

Song, F., Zhou, T., and Qian, Y.: Responses of East Asian summer monsoon to natural and anthropogenic forcings in the 17 latest CMIP5 models, Geophysical Research Letters, 41, 596–603, https://doi.org/10.1002/2013GL058705, http://doi.wiley.com/10.1002/2013GL058705, 2014.

Sperber, K. R., Annamalai, H., Kang, I.-S., Kitoh, A., Moise, A., Turner, A., Wang, B., and Zhou, T.: The Asian summer monsoon: an intercomparison of CMIP5 vs. CMIP3 simulations of the late 20th century, Climate Dynamics, 41, 2711–2744, https://doi.org/10.1007/s00382-012-1607-6, http://link.springer.com/10.1007/s00382-012-1607-6, 2013.

Swart, N. C., Cole, J. N., Kharin, V. V., Lazare, M., Scinocca, J. F., Gillett, N. P., Anstey, J., Arora, V., Christian, J. R., Jiao, Y., Lee, W. G., Majaess, F., Saenko, O. A., Seiler, C., Seinen, C., Shao, A., Solheim, L., von Salzen, K., Yang, D., Winter, B., and Sigmond, M.: CCCma CanESM5 model output prepared for CMIP6 DAMIP, https://doi.org/10.22033/ESGF/CMIP6.1305, https://doi.org/10.22033/ESGF/CMIP6.1305, 2019a.

Swart, N. C., Cole, J. N., Kharin, V. V., Lazare, M., Scinocca, J. F., Gillett, N. P., Anstey, J., Arora, V., Christian, J. R., Jiao, Y., Lee, W. G., Majaess, F., Saenko, O. A., Seiler, C., Seinen, C., Shao, A., Solheim, L., von Salzen, K., Yang, D., Winter, B., and Sigmond, M.: CCCma CanESM5 model output prepared for CMIP6 CMIP historical, https://doi.org/10.22033/ESGF/CMIP6.3610, https://doi.org/10.22033/ESGF/CMIP6.3610, 2019b.

Swart, N. C., Cole, J. N., Kharin, V. V., Lazare, M., Scinocca, J. F., Gillett, N. P., Anstey, J., Arora, V., Christian, J. R., Jiao, Y., Lee, W. G., Majaess, F., Saenko, O. A., Seiler, C., Seinen, C., Shao, A., Solheim, L., von Salzen, K., Yang, D., Winter, B., and Sigmond, M.: CCCma CanESM5 model output prepared for CMIP6 ScenarioMIP, https://doi.org/10.22033/ESGF/CMIP6.1317, https://doi.org/10.22033/ESGF/CMIP6.1317, 2019c.

Tang, Y., Rumbold, S., Ellis, R., Kelley, D., Mulcahy, J., Sellar, A., Walton, J., and Jones, C.: MOHC UKESM1.0-LL model output prepared for CMIP6 CMIP historical, https://doi.org/10.22033/ESGF/CMIP6.6113, https://doi.org/10.22033/ESGF/CMIP6.6113, 2019.

Tatebe, H. and Watanabe, M.: MIROC MIROC6 model output prepared for CMIP6 CMIP historical, https://doi.org/10.22033/ESGF/CMIP6.5603, https://doi.org/10.22033/ESGF/CMIP6.5603, 2018.

Taylor, K. E., Stouffer, R. J., Meehl, G. A., Taylor, K. E., Stouffer, R. J., and Meehl, G. A.: An Overview of CMIP5 and the Experiment Design, Bulletin of the American Meteorological Society, 93, 485–498, https://doi.org/10.1175/BAMS-D-11-00094.1, http://journals.ametsoc.org/doi/abs/10.1175/BAMS-D-11-00094.1, 2012.

Undorf, S., Polson, D., Bollasina, M. A., Ming, Y., Schurer, A., and Hegerl, G. C.: Detectable Impact of Local and Remote Anthropogenic Aerosols on the 20th Century Changes of West African and South Asian Monsoon Precipitation, Journal of Geophysical Research: Atmospheres, 123, 4871–4889, https://doi.org/10.1029/2017JD027711, http://doi.wiley.com/10.1029/2017JD027711, 2018.

van Vuuren, D. P., Edmonds, J., Kainuma, M., Riahi, K., Thomson, A., Hibbard, K., Hurtt, G. C., Kram, T., Krey, V., Lamarque, J.-F., Masui, T., Meinshausen, M., Nakicenovic, N., Smith, S. J., and Rose, S. K.: The representative concentration pathways: an overview, Climatic Change, 109, 5–31, https://doi.org/10.1007/s10584-011-0148-z, http://link.springer.com/10.1007/s10584-011-0148-z, 2011.

Voldoire, A.: CMIP6 simulations of the CNRM-CERFACS based on CNRM-CM6-1 model for CMIP experiment historical, https://doi.org/10.22033/ESGF/CMIP6.4066, https://doi.org/10.22033/ESGF/CMIP6.4066, 2018.

Voldoire, A.: CNRM-CERFACS CNRM-CM6-1 model output prepared for CMIP6 RFMIP, https://doi.org/10.22033/ESGF/CMIP6.1383, https://doi.org/10.22033/ESGF/CMIP6.1383, 2019a.

Voldoire, A.: CNRM-CERFACS CNRM-CM6-1 model output prepared for CMIP6 ScenarioMIP, https://doi.org/10.22033/ESGF/CMIP6.1384, https://doi.org/10.22033/ESGF/CMIP6.1384, 2019b.

Westervelt, D. M., Horowitz, L. W., Naik, V., Golaz, J.-C., and Mauzerall, D. L.: Radiative forcing and climate response to projected 21st century aerosol decreases, Atmospheric Chemistry and Physics, 15, 12 681–12 703, https://doi.org/10.5194/acp-15-12681-2015, https://www.atmos-chem-phys.net/15/12681/2015/, 2015.

Wilcox, L. J., Highwood, E. J., and Dunstone, N. J.: The influence of anthropogenic aerosol on multi-decadal variations of historical global climate, Environmental Research Letters, 8, 24 033, https://doi.org/10.1088/1748-9326/8/2/024033, 2013.

Wilcox, L. J., Dong, B., Sutton, R. T., and Highwood, E. J.: The 2014 hot, dry summer in northeast Asia, 96, S105–S110, https://doi.org/10.1175/BAMS-D-15-00123.1, 2015.

Wu, P., Christidis, N., and Stott, P.: Anthropogenic impact on Earth's hydrological cycle, Nature Climate Change, 3, 807–810, https://doi.org/10.1038/nclimate1932, http://www.nature.com/articles/nclimate1932, 2013.

Wu, T., Chu, M., Dong, M., Fang, Y., Jie, W., Li, J., Li, W., Liu, Q., Shi, X., Xin, X., Yan, J., Zhang, F., Zhang, J., Zhang, L., and Zhang, Y.: BCC BCC-CSM2MR model output prepared for CMIP6 CMIP historical, https://doi.org/10.22033/ESGF/CMIP6.2948, https://doi.org/10.22033/ESGF/CMIP6.2948, 2018.

Wyser, K., van Noije, T., Yang, S., von Hardenberg, J., O'Donnell, D., and D{\"o}scher, R.: On the increased climate sensitivity in the EC-Earth model from CMIP5 to CMIP6, Geoscientisic Model Development Discussions, https://doi.org/https://doi.org/10.5194/gmd-2019-282, https://www.geosci-model-dev-discuss.net/gmd-2019-282/, 2019.

Xie, P., Arkin, P. A., Xie, P., and Arkin, P. A.: Analyses of Global Monthly Precipitation Using Gauge Observations, Satellite Estimates, and Numerical Model Predictions, Journal of Climate, 9, 840–858, https://doi.org/10.1175/1520-0442(1996)009<0840:AOGMPU>2.0.CO;2, http://journals.ametsoc.org/doi/abs/10.1175/1520-0442{%}281996{%}29009{%}3C0840{%}3AAOGMPU{%}3E2.0.CO{%}3B2, 1996.

Xie, P., Arkin, P. A., Xie, P., and Arkin, P. A.: Global Precipitation: A 17-Year Monthly Analysis Based on Gauge Observations, Satellite Estimates, and Numerical Model Outputs, Bulletin of the American Meteorological Society, 78, 2539–2558, https://doi.org/10.1175/1520-0477(1997)078<2539:GPAYMA>2.0.CO;2, http://journals.ametsoc.org/doi/abs/10.1175/1520-0477{%}281997{%}29078{%}3C2539{%}3AGPAYMA{%}3E2.0.CO{%}3B2, 1997.

Xin, X., Wu, T., Shi, X., Zhang, F., Li, J., Chu, M., Liu, Q., Yan, J., Ma, Q., and Wei, M.: BCC BCC-CSM2MR model output prepared for CMIP6 ScenarioMIP, https://doi.org/10.22033/ESGF/CMIP6.1732, https://doi.org/10.22033/ESGF/CMIP6.1732, 2019.

Yatagai, A., Kamiguchi, K., Arakawa, O., Hamada, A., Yasutomi, N., Kitoh, A., Yatagai, A., Kamiguchi, K., Arakawa, O., Hamada, A., Yasutomi, N., and Kitoh, A.: APHRODITE: Constructing a Long-Term Daily Gridded Precipitation Dataset for Asia Based on a Dense Network of Rain Gauges, Bulletin of the American Meteorological Society, 93, 1401–1415, https://doi.org/10.1175/BAMS-D-11-00122.1, http://journals.ametsoc.org/doi/abs/10.1175/BAMS-D-11-00122.1, 2012.

Yukimoto, S., Koshiro, T., Kawai, H., Oshima, N., Yoshida, K., Urakawa, S., Tsujino, H., Deushi, M., Tanaka, T., Hosaka, M., Yoshimura, H., Shindo, E., Mizuta, R., Ishii, M., Obata, A., and Adachi, Y.: MRI MRI-ESM2.0 model output prepared for CMIP6 CMIP historical, https://doi.org/10.22033/ESGF/CMIP6.6842, https://doi.org/10.22033/ESGF/CMIP6.6842, 2019a.

Yukimoto, S., Koshiro, T., Kawai, H., Oshima, N., Yoshida, K., Urakawa, S., Tsujino, H., Deushi, M., Tanaka, T., Hosaka, M., Yoshimura, H., Shindo, E., Mizuta, R., Ishii, M., Obata, A., and Adachi, Y.: MRI MRI-ESM2.0 model output prepared for CMIP6 RFMIP, https://doi.org/10.22033/ESGF/CMIP6.635, https://doi.org/10.22033/ESGF/CMIP6.635, 2019b.

Yukimoto, S., Koshiro, T., Kawai, H., Oshima, N., Yoshida, K., Urakawa, S., Tsujino, H., Deushi, M., Tanaka, T., Hosaka, M., Yoshimura, H., Shindo, E., Mizuta, R., Ishii, M., Obata, A., and Adachi, Y.: MRI MRI-ESM2.0 model output prepared for CMIP6 ScenarioMIP, https://doi.org/10.22033/ESGF/CMIP6.638, https://doi.org/10.22033/ESGF/CMIP6.638, 2019c.

Zelinka, M. D., Andrews, T., Forster, P. M., and Taylor, K. E.: Quantifying Components of Aerosol-Cloud-Radiation Interactions in Climate Models, Journal of Geophysical Research: Atmospheres, 119, 7599–7615, https://doi.org/10.1002/2014JD021710, 2014.

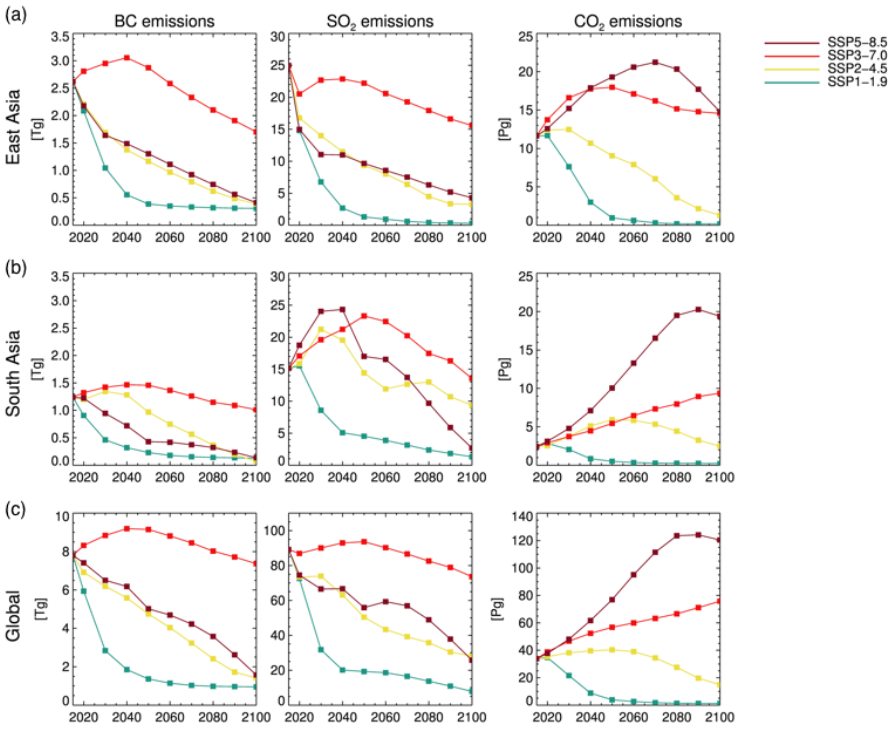

Figure 1. (a): Black carbon [Tg], (b): sulphur dioxide [Tg], and (c): carbon dioxide emissions [Pg] over East Asia for SSPs 1-19, 2-45, 3-70, and 5-85. (d)-(f): emissions over South Asia. (g)-(h): global total emissions. East Asia is the region from 20-40°N and 100-120°E~~and 20-40° N~~. South Asia is the region from ~~55-95°E and~~ 5-25°N and 55-95°E.

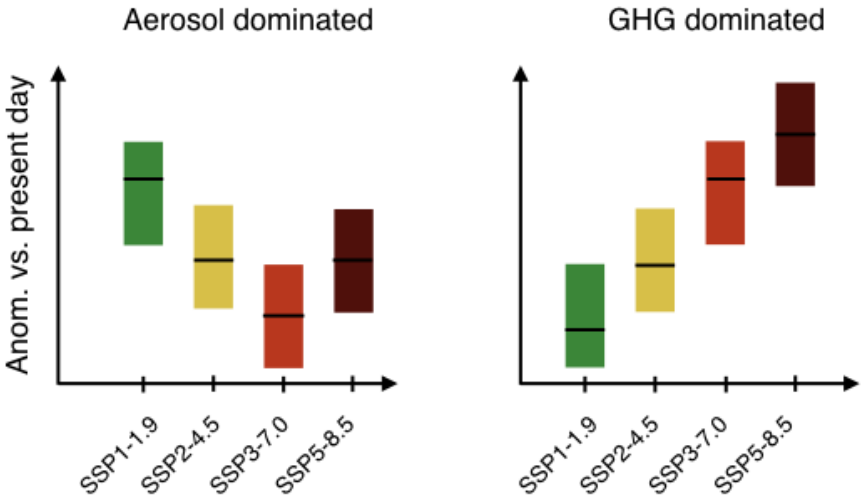

Figure 2. ~~((a): Global-mean annual-mean temperature anomaly~~ Schematics showing the anticipated pattern of anomalies relative to ~~1951-1980 from CMIP6 (grey lines show individual members) and GISTEMP (black). (b): June to August (JJA) mean interhemispheric temperature gradient anomaly relative to 1951-1980 from CMIP6 (grey) and GISTEMP. (c): Annual-mean global-mean precipitation anomaly relative to 180-2014 from CMIP6 (grey) and GPCP (black). (d): JJA-mean Asia-mean precipitation anomaly relative to~~ 1980-2014 ~~from CMIP6 (grey) and GPCP (black). (e): linear trends~~ across the SSPs in ~~annual-mean global-mean temperature~~ cases where the differences are aerosol-dominated and ~~JJA-mean interhemispheric temperature gradient from CMIP6 (coloured diamonds) and GISTEMP (grey bars) for 1950-1974 and 1980-2014~~GHG-dominated, ~~and linear trends in annual-mean global-mean precipitation and JJA-mean Asia-mean precipitation for 1980-2014. Error bars show plus or minus one standard error~~ based on the ~~observed trend~~global emission pathways shown in Figure 1c.~~Note that for Asian precipitation this extends beyond the range of the plot, and is an order of magnitude larger than the trend. Asia is the region from 67.5-145°E, and 5-47.5°N.~~

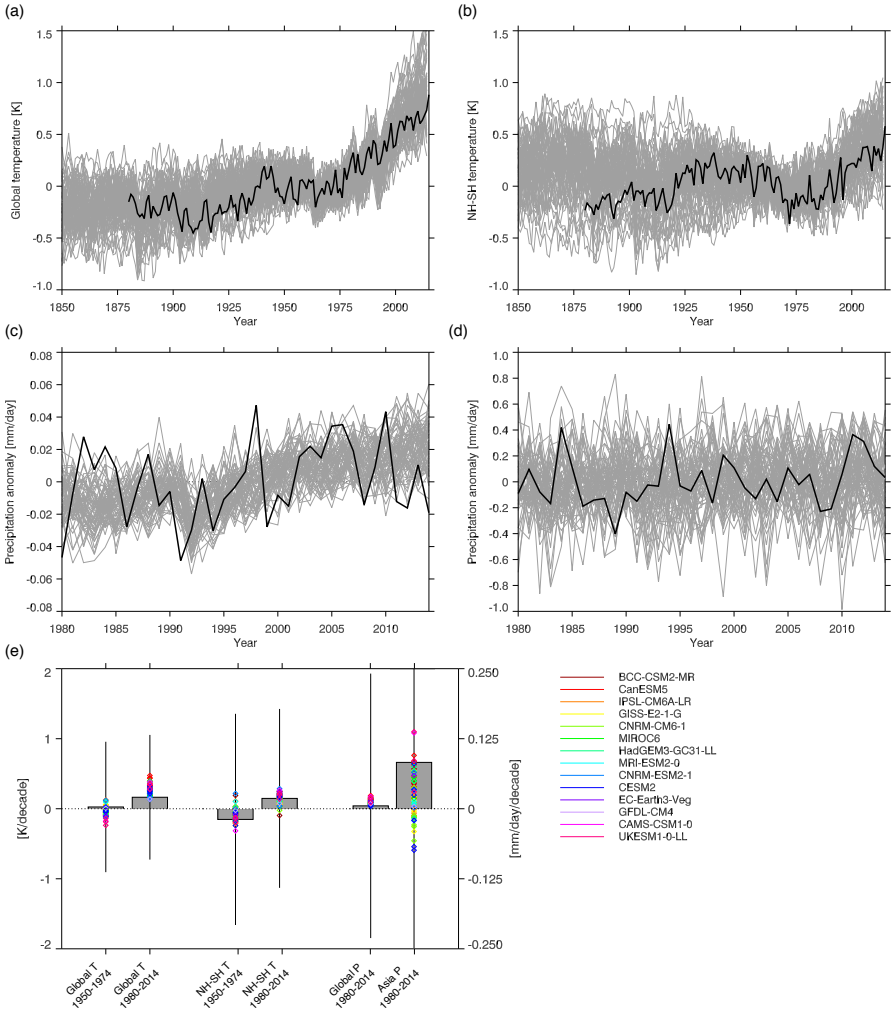

Figure 3. ((a): Global-mean annual-mean temperature anomaly relative to 1951-1980 from CMIP6 (grey lines show individual members) and GISTEMP (black). (b): Annual-mean interhemispheric temperature gradient anomaly relative to 1951-1980 from CMIP6 (grey) and GISTEMP. (c): Annual-mean global-mean precipitation anomaly relative to 1980-2014 from CMIP6 (grey) and GPCP (black). (d): JJA mean Asia-mean precipitation anomaly relative to 1980-2014 from CMIP6 (grey) and GPCP (black). Asia is the region from 5-47.5°N and 67.5-145°E. (e): linear trends in annual-mean global-mean temperature and JJA-mean interhemispheric temperature gradient from CMIP6 (coloured diamonds) and GISTEMP (grey bars) for 1950-1974 and 1980-2014, and linear trends in annual-mean global-mean precipitation and JJA-mean Asia-mean precipitation for 1980-2014 (grey bars are GPCP). Error bars show plus or minus one standard error on the observed trend. Note that for Asian precipitation this extends beyond the range of the plot, and is an order of magnitude larger than the trend.

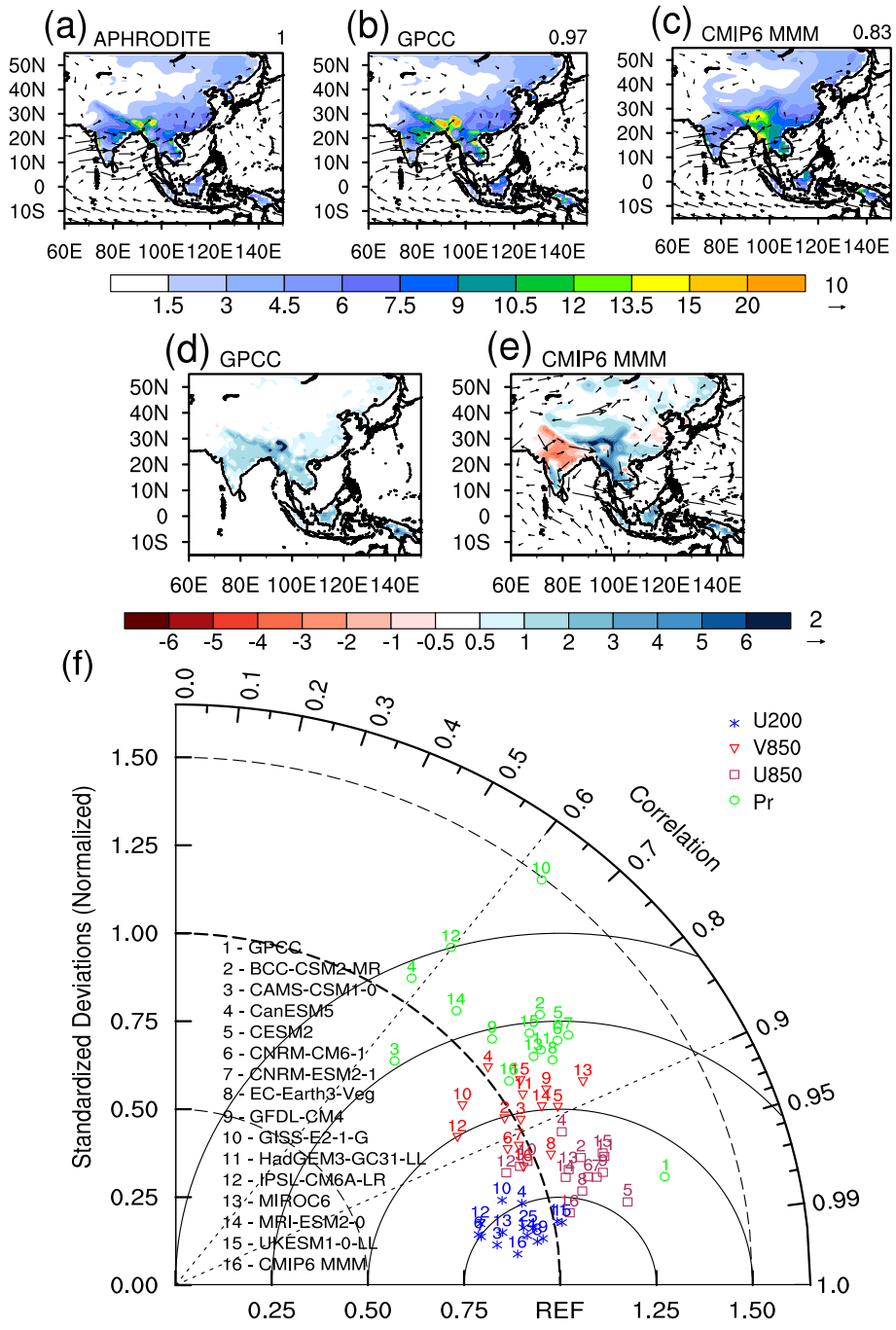

Figure 4. ~~JJAS mean~~ JJA-mean 1980-2014 mean precipitation over land [mm day^{-1}] overlaid with 850 hPa wind [m s^{-1}] from (a): APHRODITE and ERA-Interim; (b): GPCC and ERA-Interim; (c): CMIP6 (multi-model mean). Values in the top right corner of panels (a)-(c) show the pattern correlation with APHRODITE precipitation. (d): Precipitation bias in GPCC relative to APHRODITE; (e): CMIP6 precipitation relative to APHRODITE and CMIP6 850 hPa winds relative to ERA-Interim. (f): Taylor diagram showing the relationship between individual CMIP6 models, the CMIP6 multi-model mean (point 16), ~~and CMAP~~ GPCC (point 1), ~~with~~ and APHRODITE precipitation and ERA-Interim winds. ~~Model numbers within a solid square indicate the model with the smallest absolute bias for each variable.~~

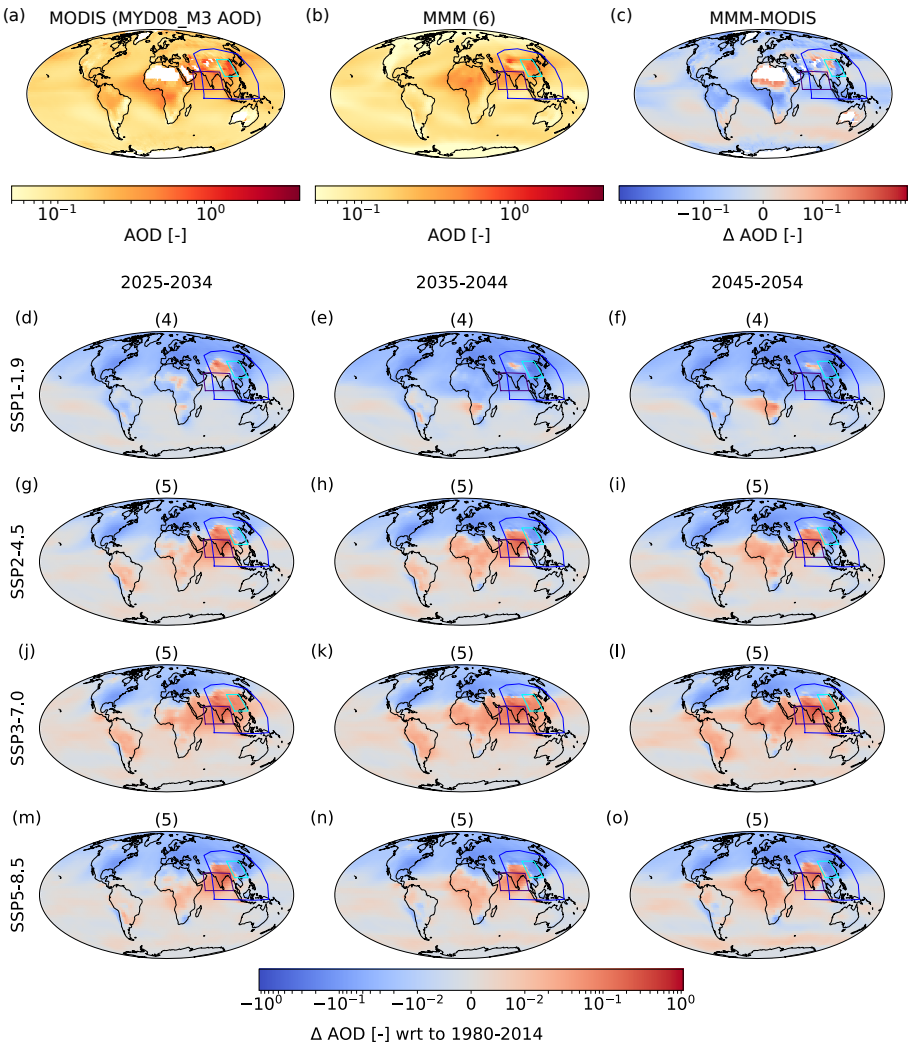

Figure 5. (a): 2002-2014 mean aerosol optical depth at 550 nm from MODIS; (b): 2002-2014 mean CMIP6 multi-model mean aerosol optical depth at 550 nm (based on 6 models (Table 1)); (c): CMIP6 bias relative to MODIS. CMIP6 AOD anomalies for 2025-2034, 2035-2044, and 2045-2054 vs. 1980-2014 for (d): SSP1-1.9; (e): SSP2-4.5; ~~and~~ (f):SSP3-7.0, and (g):SSP5-8.5. For SSP1-1.9 the anomalies are based on 4 models. For all other panels, ~~6~~ 5 models are used (Table 1). Blue, purple, and turquoise boxes show the 'Asia', 'South Asia', and 'East Asia' regions used in later analysis. Asia is the region bounded by 5-47.5°N, 67.5-145°E, East Asia is the region bounded by 20-40°N and 100-120°E, and South Asia is the region bounded by 5-25°N and 55-95°E.

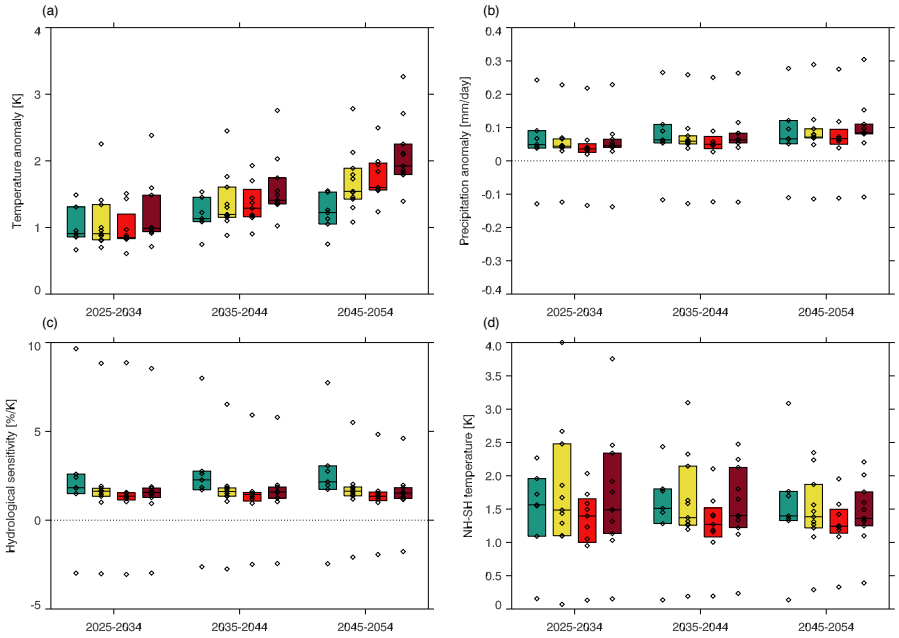

Figure 6. ~~Global mean annual mean~~ Global-mean annual-mean anomalies in (a): near-surface temperature [K]; (b): precipitation [mm ~~/~~day^{-1}]; (c): hydrological sensitivity [% ~~/~~K^{-1}] relative to 1980-2014. (d): ~~JJA~~ Annual mean anomalies in interhemispheric temperature gradient [K] relative to 1980-2014. Coloured bars show the interquartile range, and the horizontal bar within this shows the median. Diamonds show values from each model listed in Table 1 as having data availability for a given SSP. Where multiple ensemble members are available the model mean is used.

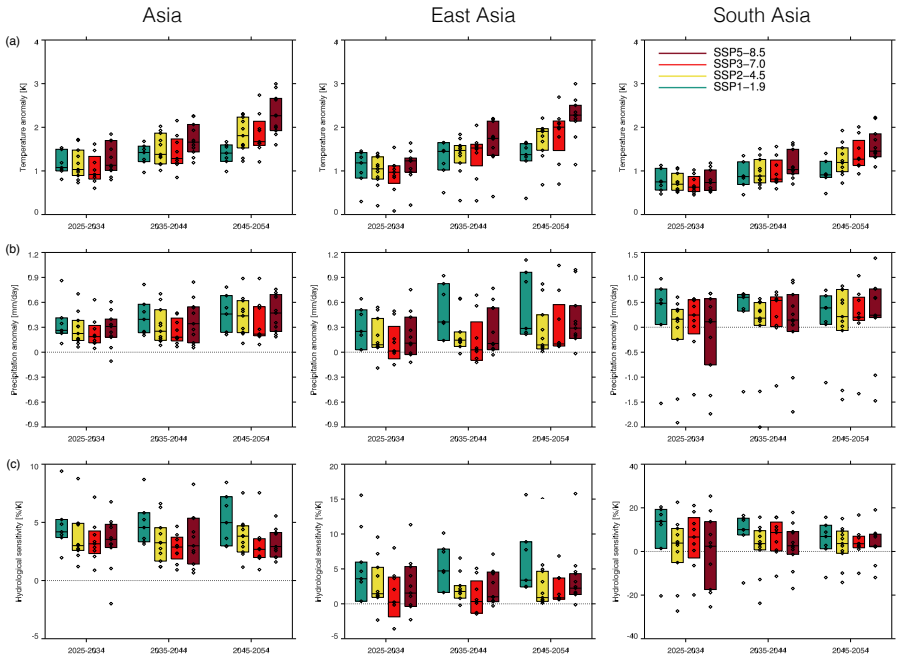

Figure 7. ~~CMIP6~~ Regional mean JJA mean temperature [K], precipitation [mm ~~/~~day^{-1}], and hydrological sensitivity [% ~~/~~K^{-1}] anomalies relative to 1980-2014 for (a): Asia; (b): East Asia; and (c): South Asia. The three regions are indicated by the boxes in Figure 5. Coloured bars show the interquartile range, and the horizontal bar within this shows the median. Diamonds show values from each model listed in Table 1 as having data availability for a given SSP. Where multiple ensemble members are available the model mean is used. Note that different y-ranges are used for each region in panels (b) and (c).

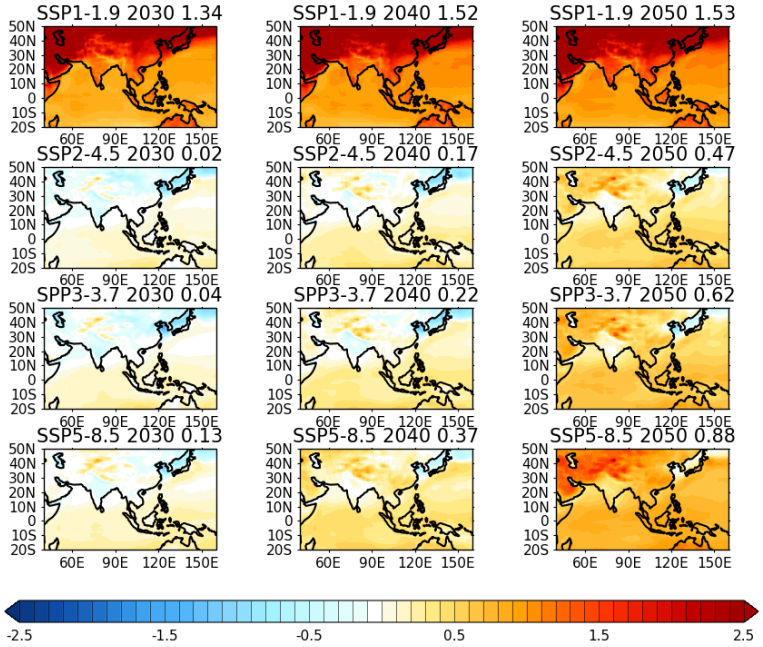

Figure 8. (a): ~~CMIP6 JJAS~~ CMIP6-mean JJA-mean near-surface temperature anomaly [K] for 2025-2034, 2035-2044, and 2045-2054 vs. 1980-2014 from SSP1-1.9. Relative anomalies for (b): ~~SSP2-45~~SSP2-4.5.; (c): SSP3-7.0; and (d): SSP5-8.5 vs. SSP1-1.9. The numbers shown at the top right of each panel are the Asian mean, where Asia is the region bounded by 5-47.5°N, 67.5-145°E.

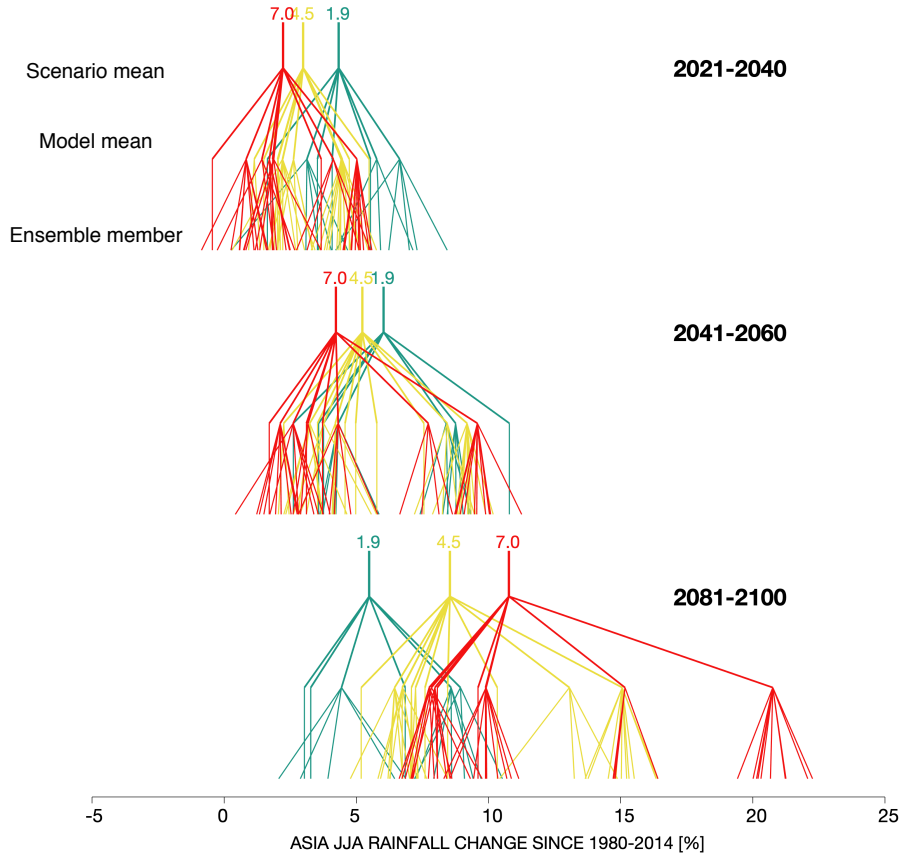

Figure 9. ~~Asia mean JJA mean~~ Asia-mean JJA-mean precipitation anomaly [%] relative to 1980-2014 in ~~individual models~~ scenario and model means, and individual ensemble members, for 2021-2040, 2041-2060, and 2081-2100, from SSP1-1.9, SSP2-4.5, and SSP3-7.0.

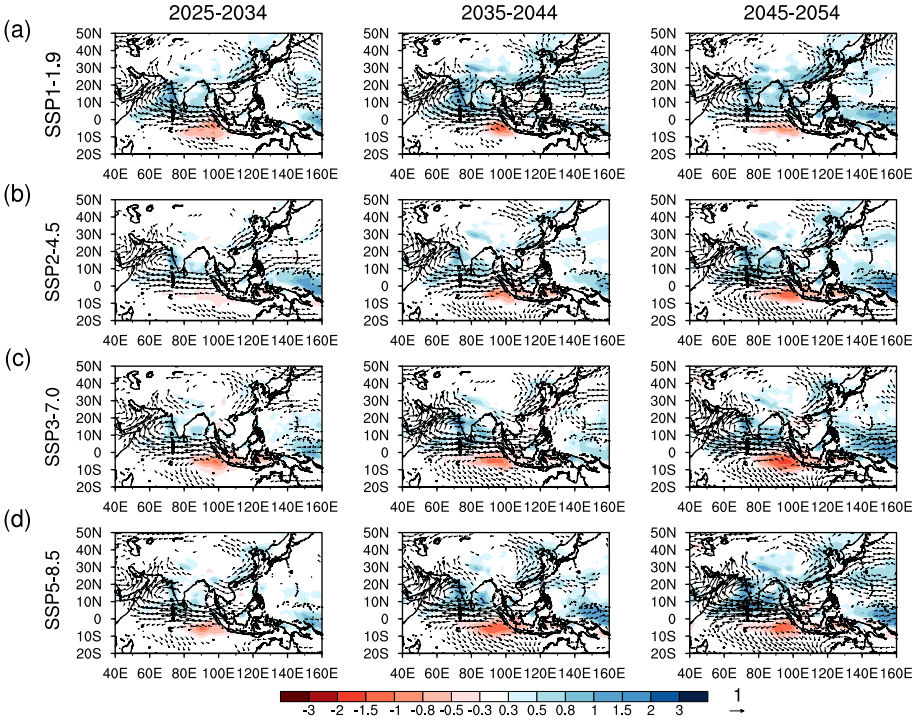

Figure 10. ~~CMIP6 JJAS~~ CMIP6-mean JJA-mean precipitation [mm day^{-1}] and 850 hPa wind anomalies [m s^{-1}] for 2025-2034, 2035-2044, and 2045-2054 vs. 1980-2014 from (a): SSP1-1.9; (b): SSP2-4.5; (c): SSP3-7.0; and (d): SSP5-8.5.

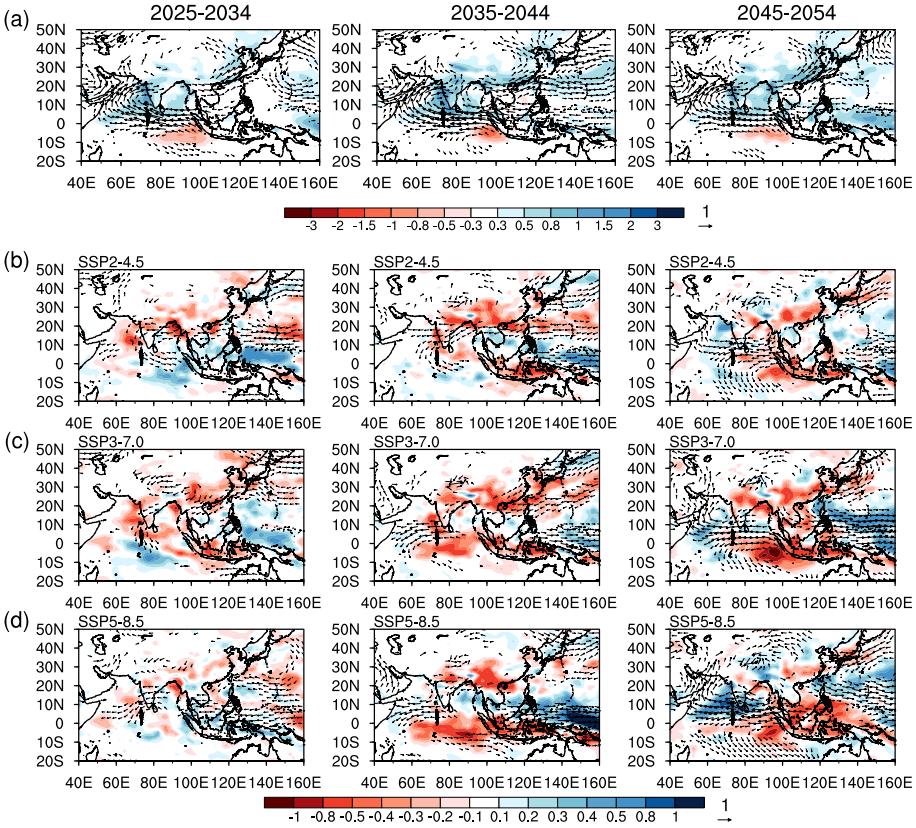

Figure 11. ~~CMIP6 JJAS~~ (a): JJA-mean precipitation [mm day^{-1}] and 850 hPa wind anomalies [m s^{-1}] for 2025-2034, 2035-2044, and 2045-2054 vs. 1980-2014 from SSP1-1.9. Anomalies from (~~a~~b): SSP2-4.5; (~~b~~c): SSP3-7.0; and (~~c~~d): SSP5-8.5 relative to the anomalies from SSP1-1.9. To enable a fair comparison of the precipitation patterns, only models with data availability for all scenarios are used (see Table 1).

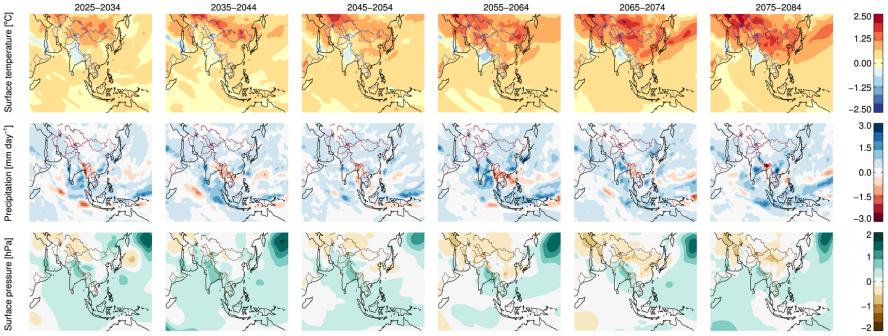

Figure 12. ~~JJAS~~ JJA-mean (a): near-surface temperature [K]; (b): precipitation [mm day^{-1}]; and (c): sea level pressure [hPa] anomalies for 10 year periods vs. 1980-2014 from an anthropogenic aerosol only version of SSP2-4.5 (SSP2-4.5-aer) with ~~CanESM5~~MIROC6.

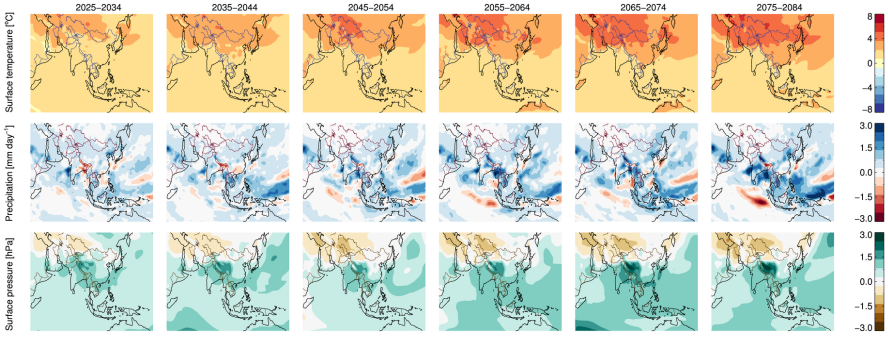

Figure 13. JJA-mean (a): near-surface temperature [K]; (b): precipitation [mm day^{-1}]; and (c): sea level pressure [hPa] anomalies for 10 year periods vs. 1980-2014 from SSP2-4.5 in MIROC6.

Table 1. CMIP6 models ~~,~~and the number of ensemble members for each ~~,~~used in this work.

		AOD					T, P, U850, and V850					Data reference
Centre	Model	hist	1-1.9	2-4.5	3-7.0	5-8.5	hist	1-1.9	2-4.5	3-7.0	~~5-8.5~~	
BCC	BCC-CSM2-MR						3		1	1	1	Wu et al. (2018); Xin et al. (2019)
CAMS	CAMS-CSM1-0						1	1	1	1	1	Rong (2019a); Rong (2019b)
CCCma	CanESM5	1	1	1	1	1	10	5	10	10	10	Swart et al. (2019b); Swart et al. (201
CNRM-CERFACS	CNRM-CM6-1	6		6	6	6	10		5	6	5	Voldoire (2018); Voldoire (2019b)
CNRM-CERFACS	CNRM-ESM2-1	5	5	5	5	5	5	5	5	5		Seferian (2018); Seferian (2019b)
EC-Earth-Consortium	EC-Earth3-Veg						1		1		1	(EC-Earth); (EC-Earth)
IPSL	IPSL-CM6A-LR	9	1	2	9	1	10	1	2	10	1	Boucher et al. (2018a); Boucher et al.
MIROC	MIROC6						3	1	3	3	3	Tatebe and Watanabe (2018)
MOHC	HadGEM3-GC31-LL						4					Ridley et al. (2019)
MOHC	UKESM1-0-LL	6	5	5	5	5	4	4	5	5	5	Tang et al. (2019); Good et al. (2019)
MRI	MRI-ESM2-0						3	1	1	1	1	Yukimoto et al. (2019a); Yukimoto et
NASA-GISS	GISS-E2-1-G						5					for Space Studies (NASA/GISS)
NCAR	CESM2	10		~~1~~	~~2~~	~~2~~	6		~~1~~	~~1~~	~~1~~	Danabasoglu (2019a)
NOAA-GFDL	GFDL-CM4						1		1		1	Guo et al. (2018b); Guo et al. (2018a)

Table 2. Historical effective radiative forcing (ERF), calculated from RFMIP sstclim experiments, and ECS from Pendergrass (2019). Models shown in *italics* are only used in historical analysis, and do not appear in Figures 6 to 10.

		ERF [W m^{-2}]			ECS	Data reference
Centre	Model	AA	GHG	LU		
CCCma	CanESM5				11.18	
CNRM-CERFACS	CNRM-CM6-1	-1.15	2.64		9.59	Voldoire (2019a)
CNRM-CERFACS	CNRM-ESM2-1	-0.74	2.41	-0.07	9.31	Seferian (2019a)
IPSL	IPSL-CM6A-LR	-0.59	2.84	-0.02	8.97	Boucher et al. (2018b)
MIROC	MIROC6	-1.06	2.69	-0.03	5.08	Sekiguchi and Shiogama (2019)
MOHC	*HadGEM3-GC31-LL*	*-1.10*	*3.09*	*-0.11*	*10.81*	*Andrews (2019)*
MOHC	UKESM1-0-LL	-1.11	2.97	-0.18	10.53	O'Connor et al. (2019)
MRI	MRI-ESM2-0	-1.19	3.03	-0.18	6.60	Yukimoto et al. (2019b)
NASA-GISS	*GISS-E2-1-G*	*-1.32*	*2.92*	*-0.00*	*5.13*	*for Space Studies (NASA/GISS)*
NCAR	*CESM2*	*-1.37*	*3.04*	*-0.04*	*10.24*	*Danabasoglu (2019b)*
NOAA-GFDL	GFDL-CM4	-0.73	3.14	-0.33	7.67	Paynter et al. (2018)